Available online at www.sciencedirect.com
ScienceDirect
Bioorganic & Medicinal Chemistry 14 (2006) 7083–7104
Bioorganic & Medicinal Chemistry

Tailoring structure–function and targeting properties of ceramides by site-specific cationization

Zdzislaw M. Szulc,[a] Jacek Bielawski,[a] Hanna Gracz,[b] Marietta Gustilo,[a] Nalini Mayroo,[a] Yusuf A. Hannun,[a] Lina M. Obeid[a,c] and Alicja Bielawska[a,*]

[a]*Department of Biochemistry and Molecular Biology, Medical University of South Carolina, Charleston, SC 29425, USA*
[b]*Department of Molecular and Structural Biochemistry, North Carolina State University, Raleigh, NC 27695, USA*
[c]*Department of Medicine and The Ralph H. Johnson Veterans Administration Medical Center, Medical University of South Carolina, Charleston, SC 29425, USA*

Received 2 May 2006; revised 29 June 2006; accepted 1 July 2006
Available online 17 August 2006

Abstract—In the course of our studies on compartment-specific lipid-mediated cell regulation, we identified an intimate connection between ceramides (Cers) and the mitochondria-dependent death-signaling pathways. Here, we report on a new class of cationic Cer mimics, dubbed ceramidoids, designed to act as organelle-targeted sphingolipids (SPLs), based on conjugates of Cer and dihydroceramide (dhCer) with pyridinium salts (CCPS and dhCCPS, respectively). Ceramidoids having the pyridinium salt unit (PSU) placed internally (α and γ-CCPS) or as a tether (ω-CCPS) in the *N*-acyl moiety were prepared by N-acylation of sphingoid bases with different ω-bromo acids or pyridine carboxylic acid chlorides following capping with respective pyridines or alkyl bromides. Consistent with their design, these analogs, showed a significantly improved solubility in water, well-resolved NMR spectra in D_2O, broadly modified hydrophobicity, fast cellular uptake, and higher anticancer activities in cells in comparison to uncharged counterparts. Structure–activity relationship (SAR) studies in MCF-7 breast carcinoma cells revealed that the location of the PSU and its overall chain length affected markedly the cytotoxic effects of these ceramidoids. All ω-CCPSs were more potent ($IC_{50/48\ h}$: 0.6–8.0 μM) than their α/γ-CCPS ($IC_{50/48\ h}$: 8–20 μM) or D-*erythro*-C6-Cer ($IC_{50/48\ h}$: 15 μM) analogs. ω-DhCCPSs were also moderately potent ($IC_{50/48\ h}$: 2.5–12.5 μM). Long-chain ω-dhCCPSs were rapidly and efficiently oxidized in cells to the corresponding ω-CCPSs, as established by LC–MS analysis. CCPS analogs also induced acute changes in the levels and composition of endogenous Cers (upregulation of C16-, C14-, and C18-Cers, and downregulation of C24:0- and C24:1-Cers). These novel ceramidoids illustrate the feasibility of compartment-targeted lipids, and they should be useful in cell-based studies as well as potential novel therapeutics.

1. Introduction

Ceramides (Cers) are long-chain amphiphilic (2*S*,3*R*, 4*E*)-2-aminoacyl-1,3-diols (Scheme 1) capable of regulating a diverse range of important cellular processes such as cell growth, differentiation, and apoptosis.[1–3] Intracellular levels of endogenous Cers are influenced by many external inducers, including cytokines (Fas, TNFα), 'environmental' stress factors (UV, radiation, hypoxia/reperfusion or hyperthermia/heat), chemotherapeutic agents (taxol, etoposide, gemcitabine or Ara-C), inhibitors of Cer metabolizing enzymes (D-MAPP, B13, PDMP), as well as by exogenously added cell membrane-permeable short-chain C2–C8-Cers.[4–13] Intracellular action of Cers on phosphatases, kinases, proteases or telomerase enzymes can be linked to their proapoptotic activities.[14–18]

However, these and other mechanistic studies with varied chain Cers revealed several major drawbacks on the SAR studies of Cers in cancer cells, limiting their potential therapeutic utility.[11,19–25] Naturally occurring Cers are highly hydrophobic, poorly water-soluble molecules, with a limited cell membrane permeability resulting in their inefficient delivery into the cells and tissues.[26–30] Improvement in the delivery of long-chain ceramides to the cells was achieved by using a solvent of ethanol containing 2% dodecane or decane showing that natural Cer could induce apoptosis.[31] This has been cited as direct evidence for the role of natural Cer in cellular

Keywords: Ceramide; Cationic ceramides; Ceramidoids; Ceramide conjugates with pyridinium salts; CCPS-analogs; Synthesis; LC–MS; NMR; Cytotoxicity.
* Corresponding author. Tel.: +1 843 792 0273; fax: +1 843 792 4322; e-mail: bielawsk@musc.edu

0968-0896/$ - see front matter © 2006 Elsevier Ltd. All rights reserved.
doi:10.1016/j.bmc.2006.07.016

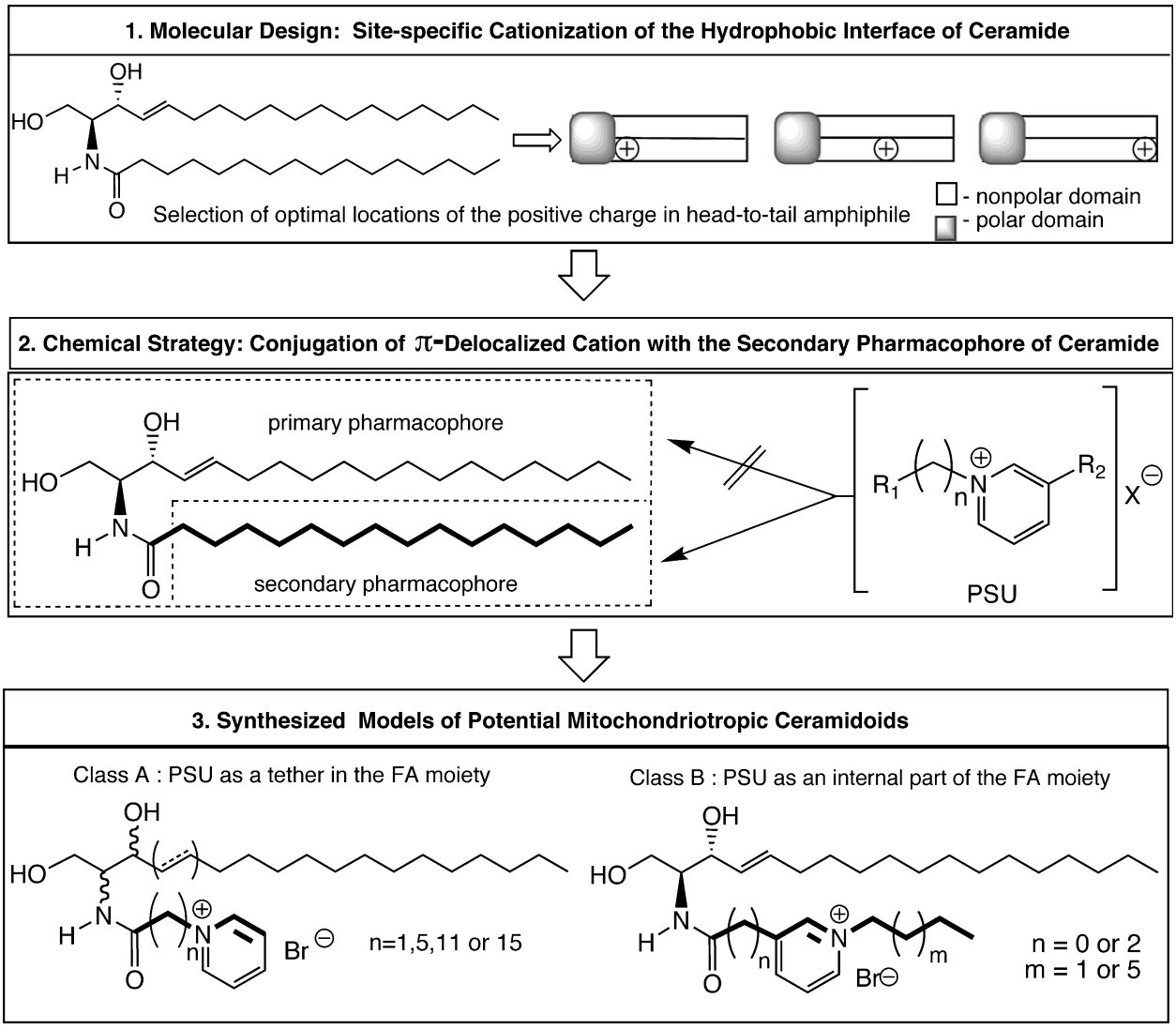

Scheme 1. Design of ceramidoids and conjugation scheme for the linkage of pyridinium cation to ceramide.

apoptosis.[32,33] However, the following studies by Tsering and Griffin did not support the above concept showing that intact long-chain Cer did not initiate cell toxicity, and rather a metabolite derived from Cer degradation may be responsible for this process.[34] Also the study by Urbina et al. showed that alkanes are not innocuous vesicles for long-chain Cer in cell biology studies causing the inhibition of Cer-dependent membrane permeabilization.[35] Short-chain Cers can be delivered into the cells, but no organelle-specific targeting was observed (except for the predominant localization of NBD-C6-Cer to the Golgi apparatus).[36,37] Recently, in order to overcome some of these limitations, liposomal formulations of Cers were developed and used in vitro and in vivo in anticancer studies.[38–41] However, several restrictions, especially for the long-chain Cers, were noticed, and these formulations resulted only in a moderate increase of their potency without any tumor tissue specificity.[38,40,41] Moreover, it is becoming increasingly apparent that accumulation of endogenous Cers in response to a variety of agonists occurs in specific sub-cellular compartments, and, thus, these compartmentally restricted Cers may play distinct roles in mediating agonist responses, depending on the compartmental formation and action.[42,43]

To address the above issues and to improve delivery and targeting properties of Cers, we designed charge-dependent organelle-targeted Cers, dubbed ceramidoids. As an initial aim, we focused on the development of ceramidoids with a fixed positive charge. This electronic feature would allow their targeting and delivery into negatively charged cellular organelles as mitochondria and/or nucleus.[44] Targeting mitochondria was our primary goal since increasing evidence is beginning to point on mitochondrial action of Cers and other SPLs.[18,45,46] Indeed, recent studies show that specific generation of Cer in mitochondria results in apoptosis and that mitochondrial Cer may drive the translocation and 'activation' of the pro-apoptotic Bax molecule.[46,47] Moreover, the other specific mitochondrial functions of Cers as formation of channels in membranes,[48] regulation of the respiratory chain proteins,[49] and release of cytochrome C have been established.[46,50]

It is well known that lipophilic and π-electron delocalized cations localize preferentially into mitochondria, and the balance between charge and the hydrophobic effects appears to be essential for their optimized mitochondrial localization.[51–54] Structurally diversified compounds: antioxidants, vitamins, fluorescent ligands, and non-viral transfecting agents, have been re-designed based on these principles to develop selective mitochondriotropic molecular probes and potential drugs.[55–60]

Therefore, we selected to synthesize Cers conjugated with pyridinium salt (CCPS analogs) with the expectation that this water-solubilizing handle will result in their improved delivery to cancer cells and selective accumulation in mitochondria due to lipophilic partitioning and trans-membrane potential-driven electrophoresis.[51,57,58,61]

Here we describe the design and synthesis of these novel cationic Cer mimics. Also, we define their basic physicochemical and biological properties: solubility in water, molecular hydrophobicity, NMR spectral behavior, including spectra recorded in D_2O, and cytotoxic effects in MCF7 cells. Additionally, we show regulatory effects of these analogs on endogenous Cer species.

We believe these results are sufficient prerequisites for the selection of lead compounds for further structural and mechanistic in vitro and in vivo studies aimed to explain anti-proliferative activity of Cer on a molecular level.

2. Results and discussion

2.1. Chemistry

2.1.1. Design of ceramidoids. The following rationale was used to design the mitochondriotropic Cers: (i) the *N*-acyl moiety of Cers is a straightforward and accessible site for structural modifications and more accommodating for modifications since it appears to be less critical than the sphingosine (Sph) backbone which plays a crucial role in their molecular recognition,[62,64] (ii) site-specific cationization of the hydrophobic domain present in the amphiphilic ligands changes their interfacial properties and activity profiles,[61,62,65–67] (iii) the PSU is commonly used as a stable, compact, chain-compatible, non-hydrogen bond donor or acceptor, biogenic water-solubilizing and cell membrane-penetrating handle,[58,61,65–68] and (iv) the introduction of this cationic handle is simple, efficient, and versatile.[61,66,69–72]

Therefore, we synthesized one C6-Cer mimic having the PSU conjugated to another aromatic ring via a vinyl linker (**LCL186**) and a few analogs without this conjugation (**LCL29**, **124**, and **143**; Scheme 2). This extended

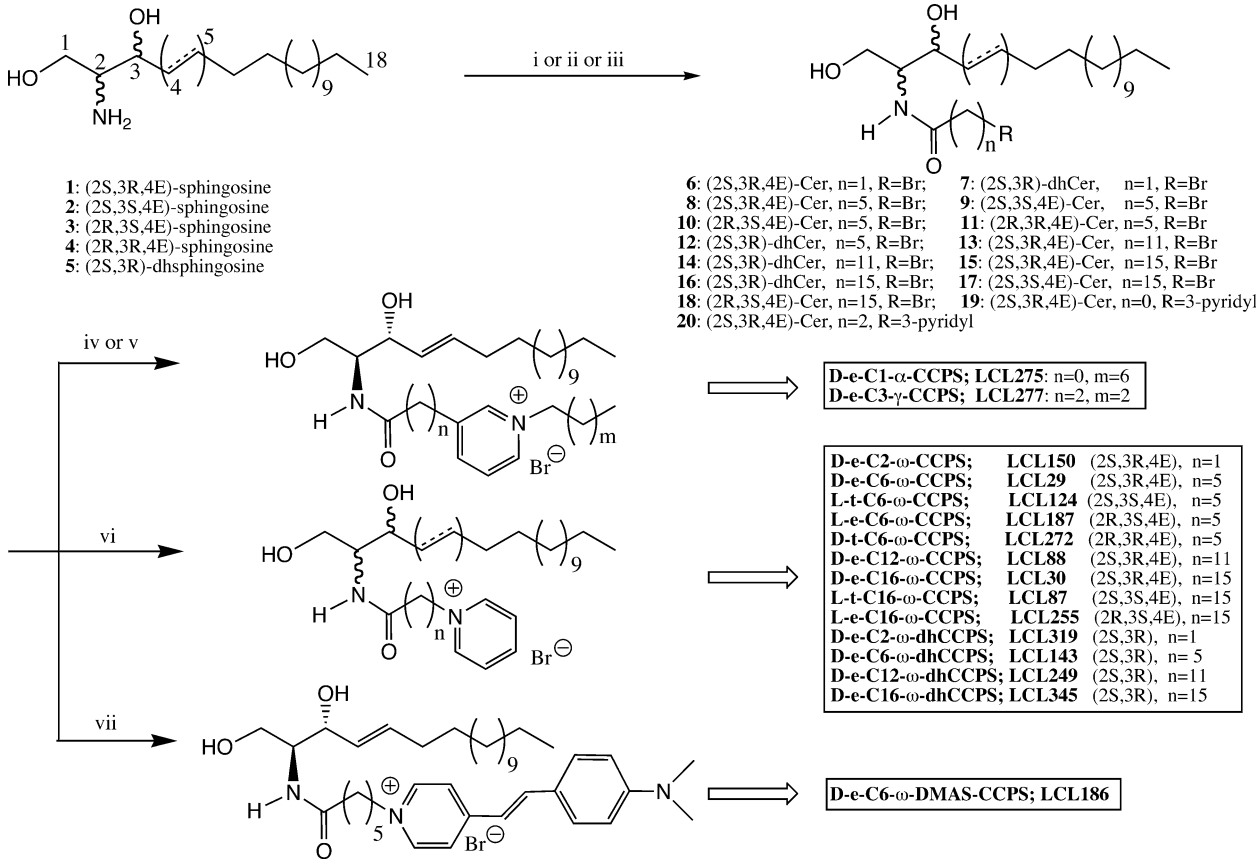

Scheme 2. Reagents and conditions. (i) $Br(CH_2)nCOX$, where n = 1, 5, 11 or 15 and X = Br or Cl, 50% CH_3COONa, THF, rt; (ii) nicotinoyl acid chloride, 50% CH_3COONa, THF, rt; (iii) 3-pyridinepropionic acid chloride, 50% CH_3COONa, THF, rt; (iv) octyl bromide, toluene, 100 °C, 12 h; (v) butyl bromide, toluene, 100 °C, 6 h; (vi) pyridine, toluene, 75–85 °C, 4–6 h; (vii) 4-[4′-(*N*,*N*-dimethylamino)styryl]-pyridine, toluene, 75–85 °C, 70 h.

conjugation of rings generates a fluorescent tag, which is itself known as a classical mitochondrial stain (DASPEI).[59] **LCL186** and its non-fluorescent analog **LCL29** localized preferentially in mitochondria of living cells, interfered with vital functions of mitochondria, and caused cancer cell death more efficiently then C6-Cer.[73] Preferential localization of other non-fluorescent analogs to mitochondria was also shown under the collaborative projects using two different sub-cellular fractionation methods and MS analysis.[74–76]

These results prompted us to design a library of CCPS analogs for SAR studies to put forward a striking hypothesis that site-specific cationization of Cer can tune its targeting properties with enhanced anticancer activity.

Thus, we designed two classes of CCPS analogs having their head-to-tail amphiphilic interfaces modified by varied locations of the PSU (Schemes 1 and 2). Class A represents Cer and dhCer analogs where the PSU functions as a tether (ω-CCPS and ω-dhCCPS). Class B represents Cer analogs where the PSU is located either in the vicinal (α-CCPS) or in the juxtaposition (γ-CCPS) to the carbonyl group. These types of conjugations warrant a placement of the positive charge in the geometrical center of the *N*-acyl chain, at a close proximity to the polar head and at the end of the Cer tail, while adjusting the chain length only.

We expected that the selected CCPS models will facilitate investigation of the influence of the key structural features of Cer, including: (i) chain length of the *N*-acyl part, (C2, C6, C12, and C16 homologs), (ii) its stereochemistry at the C2 and C3 positions of sphingoid-backbone (isomers: 2*S*, 3*R*; 2*S*, 3*S*; 2*R*, 3*S*; and 2*R*, 3*R*), and (iii) level of saturation/desaturation at the C4–C5 positions on their physicochemical and biological properties under physiological conditions.

2.1.2. Synthesis of CCPS analogs. The synthesis of target compounds was carried out efficiently according to the procedures presented in Scheme 2. Two parallel approaches, based on the previously reported protocols for the preparation of varied chain Cers from sphingoid bases[62] and quaternary salts from azines,[69–72] were developed to synthesize 1-, 1,3- and 1,4-pyridinium salt-substituted hybrid SPLs.

The first approach, designed for the preparation of class A of CCPS lipids, started with the N-acylation of **1**–**5** with ω-bromo acid chlorides. This reaction, performed in a bi-phasic solvent system of 50% aqueous solution of CH_3COONa/THF, proceeded very fast (15–25 min) and with a complete consumption of the starting sphingoid bases to give ω-bromo-Cers **6**–**12** in high yields (vide infra). Synthesis of C12 and C16 homologs required freshly prepared ω-bromo-dodecanoic and hexadecanoic acid chlorides. Initial attempts to obtain the long chains ω-bromo-Cers **14** and **15** by the condensation of **1** with the activated forms of the corresponding C12- or C16-fatty acids (i.e. NHS-esters, Imd-derivatives, etc., synthesized separately or generated in situ) were not successful (incomplete reactions, complex mixture formation, and low yields). Subsequent quaternization of pyridine or its 4-*N*,*N*-dimethylaminostyryl derivative with ω-bromo-Cers **6**–**18**, performed in toluene solution at 75–80 °C, gave the expected CCPS analogs: **LCL29**, **30**, **87**, **88**, **89**, **124**, **143**, **150**, **186**, **187**, **249**, **255**, **272**, **319**, and **345**. Synthesis of **LCL30** was selected as a model process for optimization and scaling-up. Specifically, when this process was performed on a mg (0.17 mmol) and a gram (3.7 mmol) scale, the target compound was obtained in 80% and 85% overall yields, respectively.

In order to prepare class B of CCPS lipids, the pyridine moiety was introduced first into the SPL structure, followed by its further quaternization with the selected alkyl halides. Thus, N-acylation of **1** with 3-pyridinepropionic or nicotinic acid chlorides gave ω-pyridino-Cers **19** and **20**, which were next N-alkylated with *n*-butyl or *n*-octyl bromides to afford **LCL275** and **277**, respectively. As expected, due to the presence of steric hindrance effects related to pyridine-derived substrates,[77] the effectiveness of the quaternization reactions for class B was ~20% lower as compared to class A (except for LCL186). Simply, the bulky SPL part in pyridines **19** and **20** more efficiently covers the heterocyclic nitrogen atom against the attack of an alkyl halide than the bromine atom in **6**–**18** against pyridine itself, causing a partial umbrella effect.[72,78] The observed diminished reactivity of **19** and **20** resulted in a prolonged N-alkylation time causing their gradual decomposition.

In summary, these two complementary synthetic approaches developed here are convenient and amenable for scaling-up the practical processes to deliver a structurally diversified set of CCPS analogs in good to excellent overall yields (50–85%).

All synthesized compounds were fully characterized by spectroscopy methods (MS, NMR, optical rotation) and elemental analysis (see Section 4).

As studied, the selected CCPS homologs: **LCL29**, **30**, **88**, and **150** proved to be stable under aqueous conditions at pH 4.5, 7.5, and 8.5 at 40 °C since neither their decomposition nor changes in the concentration levels over the period of 48 h were observed (RP TLC and LC–MS analysis, data not shown).

2.1.3. Physicochemical properties of CCPS analogs

2.1.3.1. Water solubility. Naturally occurring long-chain Cers are highly hydrophobic non-swelling lipids showing a marginal solubility in water in comparison to the commonly used short-chain homologs.[26–30] Comparison of the reported critical micelle concentrations (CMC) data for C2- and C6-Cers (5.0 and 6.0 μM, respectively)[28] with their water solubility (Table 1, 29.0 and 3.6 μM, respectively) indicates a preferential disposition on the air–water interface and formation of micelles. Contrary to this, C16-Cer exhibits no detergent-like properties and forms a condensed film.[27,30] Due to the tight packing properties of C16-Cer,[26] this lipid

Table 1. Solubility of the selected ceramides and CCPS analogs in water at 22 and 37 °C

Ceramides and ceramidoids	Solubility at 22 °C [mg/mL] (mM)	Solubility at 37 °C [mg/mL] (mM)
C16-Cer	ND	0.0003(0.0005)
C6-Cer	ND	0.0014(0.0036)
C2-Cer	ND	0.01(0.029)
LCL345	0.3(0.42)	1.4(2.0)
LCL30	0.5(0.72)	2.8(4.0)
LCL87	0.8(1.2)	3.6(5.2)
LCL319	0.9(1.8)	45(90)
LCL150	1.2(2.4)	82(164)
LCL275	62(103)	120(200)
LCL88[a]	34(53)	495(773)
LCL277[a]	310(544)	ND
LCL29[a]	715(1290)	ND
LCL124[a]	845(1521)	ND

ND, not determined due to the extremely low or high level of lipid solubility.

[a] These lipids form dense colloidal suspensions at the higher concentrations as reported.

easily precipitates from the aqueous solution at concentrations higher than 0.5 μM (500 pmol/mL).

As shown in Table 1, a dramatic increase in solubility in water was observed upon conjugation of Cers with the PSU. In general, the observed solubility levels for D-*e*-C2-, C6-, and C16-ω-CCPS homologs were between 4 and 6 orders of magnitude higher than for the corresponding Cers. This trend correlates with the reported data on the solubility enhancement when the PSU was used as a water-solubilizing handle for other hydrophobic compounds.[61] Specifically, at room temperature, D-*e*-C16-ω-CCPS and D-*e*-C6-ω-CCPS reached concentrations of 0.72 mM and 1.3 M, respectively. Solubility levels for D-*e*-C6- and C12-ω-CCPS at 22 °C (715 and 34 mg/mL, respectively) were significantly higher than solubility assessed for the C2-homolog (1.2 mg/mL at 22 °C and 42 mg/mL at 37 °C) as well as for the C16-homolog (0.5 mg/mL at 22 °C and 2.8 mg/mL at 37 °C). D-*e*-C6-ω-CCPS isomers showed the highest solubility in water among all studied lipids. This phenomenon is most likely due to the unique location of the positive charge in the geometrical center of the Cer structure (i.e., below the C9 atom of the C18-Sph backbone). Central placement of the PSU precludes any self-association of Cer molecules along their *N*-acyl or Sph-backbone chains, regardless of the possible arrangements of the polar heads. Moreover, this location of charge may also extend polar interface of Cer due to a possible hydration of the PSU vicinity.[79]

Surprisingly, the biggest and the most hydrophobic CCPS analog, D-*e*-C16-ω-dhCCPS (0.3 mg/mL or 0.4 mM), revealed to be more soluble in water than its non-charged congeners *N*-palmitoyl-serinol (S16, 0.17 mg/mL)[80] and galactosyl-C6-Cer (0.1 mM).[81] Coincidentally, the solubility level of D-*e*-C16-ω-CCPS at room temperature is almost identical to that reported for cetyl pyridinium bromide (CPB; 0.6 mg/mL).[82] These results indicate that Coulombic repulsions between CCPS molecules can sufficiently counterbalance their attractive interactions in water. Thus, site-specific cationization overcomes better self-association of Cer in water then its glycosylation and/or reduction of hydrocarbon chains. Placement of the positive charge in the Cer structure as well as lipid overall size revealed to be the key features affecting solubility of CCPS analogs in water. However, some environmental factors as temperature,[82] ionic strength of the solution, and a kind of the counter anion may influence their solubility either. Therefore, the assessment of these factors is currently in progress aiming at selecting a proper formulation of CCPS analogs for in vivo studies.[75]

Surprisingly, the observed decreasing order in solubility of CCPS analogs: **LCL29 > LCL275 > LCL88 > LCL150 > LCL30** does not comply with the increased length of the *N*-acyl moiety. **LCL150**, the smallest and theoretically the most polar compound, was expected to be the best water-soluble analog. To explain such a peculiar trend, and to correlate the influence of the positive charge on other biophysical properties of Cers, we investigated the molecular hydrophobicity indexes of the pertinent CCPS analogs.

2.1.3.2. Molecular hydrophobicity. Molecular hydrophobicity (R_M) is used to correlate the surface activity of amphiphilic ligands with their polarity. This property of surfactants influences also their CMC values, solubility in water, and lipid membrane permeability.[65,67]

As shown in Figure 1 the R_M values of CCPS analogs paralleled their *N*-acyl chain length, however, the R_M values for D-*e*-C6- and C12-ω-CCPS were very close (R_M = 0.19 and 0.21, respectively). The level of polarity depended on the saturation level and stereochemistry of the Sph backbone; although, the influence of the saturation was more pronounced. Interestingly, the observed differences between the R_M values of ω-CCPS and their corresponding ω-dhCCPS analogs were almost identical regardless of their chain lengths ($\Delta R_M = 0.2 \pm 0.02$). In order to evaluate the influence of the structural factors on hydrophobicity, we compared the R_M values of

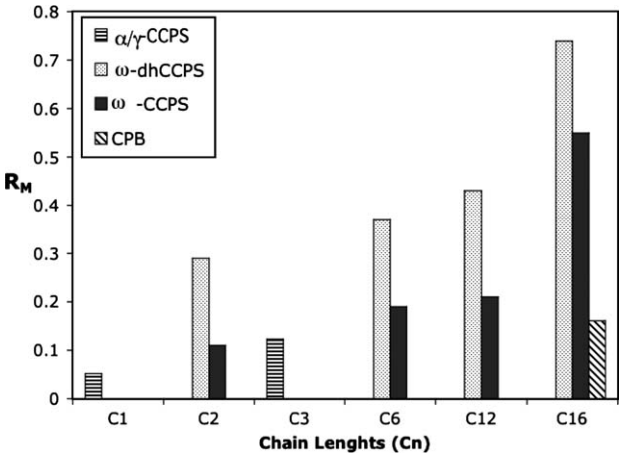

Figure 1. Effects of the linker length (Cn) between the 2-N atom of the amide group and the pyridinium ring of α/γ-CCPSs and ω-CCPSs on their molecular hydrophobicity (R_M) in comparison to CPB.

CCPS analogs with data obtained for CPB. The following increasing order of hydrophobicity was observed: **LCL275** < **LCL150** < **LCL277** < CPB < **LCL29** < **LCL124** ~ **LCL88** < **LCL-319** < **LCL143** < **LCL249** < **LCL87** < **LCL30** < **LCL345**. These results indicate that CCPS polarity depended primarily on the distance of the PSU from the polar head of Cer but not on the chain length attached to the pyridinium nitrogen atom (i.e., $NHCO(CH_2)_n$-PSU linker length). For example, the R_M value for **LCL277** ($n = 2$) is two times higher than that of **LCL275** ($n = 0$) in spite that its *N*-pyridinium-linked chain is twice shorter.

Contrary to this, **LCL29**, **LCL277**, and CPB, surfactants having varied arrangements of the PSU in chains, showed almost the same level of hydrophobicity (0.19, 0.12, and 0.16, respectively) but a different solubility in water (715, 310, and 0.6 mg/mL at 22 °C, respectively). Moreover, **LCL150** and **275**, the most polar CCPS analogs, expected to be the best soluble compounds in water, had only a moderate solubility (1.2 and 62 mg/mL, respectively). The best soluble CCPS analogs had a moderate hydrophobicity and a central location of the PSU in the Cer structure (**LCL29** and **124**).

These results indicate a complex correlation between hydrophobicity of CCPS analogs and their solubility in water. This peculiar behavior of CCPS lipids can be explained by detailed study of their differences in the aggregate morphology.[67] In conclusion, no simple correlation between R_M values and water solubility of CCPS analogs against their *N*-acyl chain lengths could be discerned.

2.1.3.3. NMR studies of a site-specific cationization of Cer. Cationization of Cers decreased the dielectric gap between Cer and water, and turned them into water-soluble compounds. This opened an unprecedented opportunity for in-depth NMR studies of Cers under physiological conditions. Here we present only selected NMR data to provide a spectroscopic proof-of-the-concept for the designed ceramidoids. Analysis of stereochemical factors governing molecular recognition of Cer by enzymes[62–64] and the reported data on its conformational preferences in aprotic solvents[83] pointed to the polar head of lipid as a primary source of information for the NMR-driven structure–biology relationship studies.[84] Also, this region includes an informative NMR paradigm: the methylene protons located at the prochiral center in a chiral molecule (Fig. 2A). The chemical shift difference for these protons which can be controlled by the magnetic non-equivalence of the surrounding environment and can be used, as an NMR benchmark, to study conformational preferences and absolute configurations in complex cyclic and acyclic chiral compounds was reported recently.[62,83,85–88]

The objective of this study was to investigate the NMR spectra of Cer in water using CCPS analogs and to determine the influence of the location of the PSU on Cer conformation. To address this issue, we recorded spectra of the selected CCPS analogs in $CDCl_3$ CD_3OD and D_2O, and compared them with the spectra of the corresponding Cers in $CDCl_3$ and CD_3OD. This set of solvents provides the environment of a wide scale of solvophobicity. The calculated ratio of the cohesive energy density (CED) values for these solvent is as follows 6:2.6:1 (with respect to H_2O, CH_3OH, and $CHCl_3$).[89] This environment may warrant a different proton-donor/proton-acceptor bond formation capability for Cer, mimicking its binding to the putative receptor.[62–64]

All CCPS analogs gave sharp and well-resolved ^1H and ^{13}C NMR spectra at 25 and 37 °C in D_2O, when using 2–10 mM samples, except for **LCL30** and **LCL345** at 25 °C. This allowed for the complete assignments of the protons and not overlapping carbon resonances using 2D ^1H–^1H-COSY and 2D ^1H–^{13}C-HMQC experiments (Figs. 2B–D and Section 4). Coupling constants for the diastereotopic 1-$H_{A,B}$ protons of Cers and CCPSs are shown in Table 2. Under varied polarity conditions, no effects of the *N*-acyl chain lengths of Cers on the chemical shift and the coupling constant values of the protons located in their polar heads were noticed, except for the C2-Cer.

2.1.3.4. Anisochronism of 1-$H_{A,B}$ protons in Cers and CCPSs, and effect of PSU on polar head conformation. To allocate ligands around the chiral centers of Cer, we used its postulated predominant (-sc)-rotamer (Fig. 2A, II).[83] Dynamic NMR studies of varied chain Cers (Table 2, Fig. 2B, see Section 4) and the reported data indicated that the chemical shift non-equivalence for the two methylene 1-$H_{A,B}$ protons ($\Delta\delta_{1\text{-HA,B}} = 0.26$–$0.22$ ppm in $CDCl_3$) was controlled by the environmental conditions.[83,85] Specifically, these protons gave a set of a two dd in $CDCl_3$ and showed a characteristic pattern for the ABX spin system with a large geminal $J_{1\text{-HAB}}$ (11.3 Hz) and a low vicinal $^3J_{2\text{-H-1HAB}}$ (3.0–3.9 Hz) coupling constants.[90] These multiplets collapsed to a one doublet ($J = 5$ Hz) in C6-, C12-, and C16-Cers or changed to the partially overlapped dd in C2-Cer ($\Delta\delta_{1\text{-HA,B}} = 0.02$ ppm, $J_{2\text{-H-1HA}} = 4.3$ and $J_{2\text{-H-1HB}} = 6.2$ Hz, respectively; Table 2) when spectra were recorded in CD_3OD. Similar patterns of changes were reported when NMR spectra of Cers were recorded in DMSO-d_6 solution.[83] These data indicate that (-sc)-conformer of D-*erythro*-Cer can easily switch from its cyclic form III to the acyclic form I in a proton-donor/acceptor solvent system (Fig. 2A). Formation of a locked (-sc)-conformation of the polar head of Cer and an asymmetric disposition of the ligands at the C2 carbon was responsible for the observed anisochronism of the 1-$H_{A,B}$ protons. In this situation, the low-field resonance signal having a higher $^3J_{2\text{-H-1HA}}$ value (*anti*-position to the 2-H proton, assigned to pro-*R* configuration) experienced a stronger shielding effect induced by the anisotropic amide carbonyl group than its pro-*S* counterpart (Fig. 2A, III). The diastereotopic 1-$H_{A,B}$ protons of all CCPS analogs showed a magnetic non-equivalence, the same type of multiplicity, and a comparable coupling constant value as were observed for the parent Cers in $CDCl_3$ solution. These data suggest that CCPS analogs adopt the same (-sc)-conformation under hydrophobic and aprotic conditions. Formation of that conformer

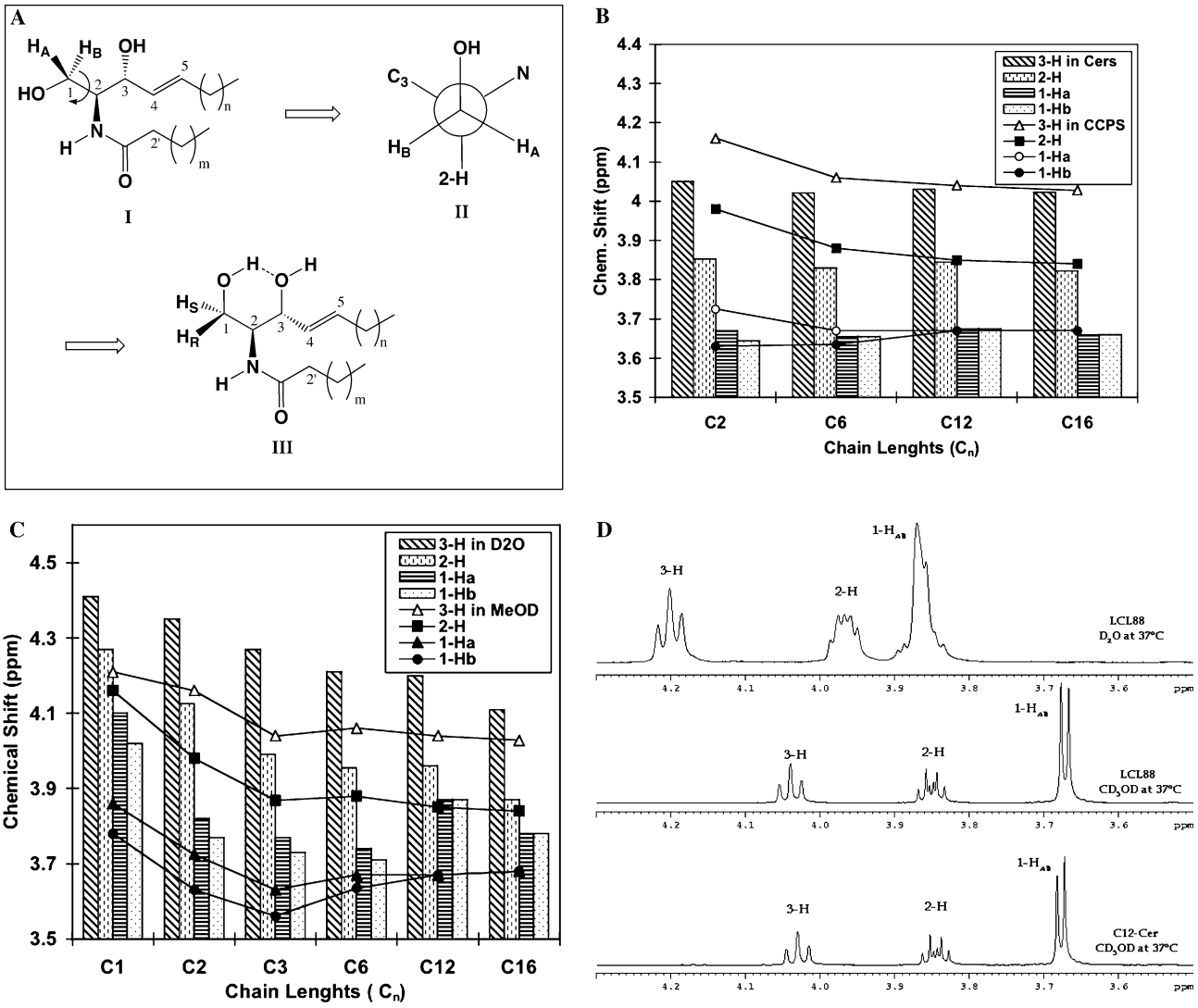

Figure 2. Spectral behavior of CCPS analogs. (A) Projection of the staggered (-sc)-conformer of D-*erythro*-Cer (**II**) showing its two diastereoscopic methylene protons 1-H_A/1-H_B (**I**) and a postulated optional cyclic conformation of the polar head having the low field proton assigned to pro-*R* and the high field proton to pro-*S* configurations (**III**). (B) Correlation of the chemical shift values of the head group protons of ω-CCPSs and the corresponding Cers against their chain lengths, shown in CD_3OD at 37 °C. (C) Correlation of the chemical shift values of the polar head protons of ω-CCPS and α/γ-CCPS in regard to the chain length distance between the 2-N atom of the NHCO group and the PSU, shown in D_2O and CD_3OD at 37 °C. (D) ^1H NMR spectra of the polar head protons of D-*e*-C12-ω-CCPS (**LCL-88**) in D_2O and CD_3OD in comparison to D-*e*-C12-Cer in CD_3OD.

Table 2. ^1H–^1H Coupling constants measured in Hz for the methylene protons 1-H_A and 1-H_B of CCPSs and ceramides, shown in different solvents at 37 °C

Compound	$CDCl_3$			CD_3OD			D_2O		
	$^3J_{2H\text{-}1HA}$	$^3J_{2H\text{-}1HB}$	J_{1HAB}	$^3J_{2H\text{-}1HA}$	$^3J_{2H\text{-}1B}$	J_{1HAB}	$^3J_{2H\text{-}1HA}$	$^3J_{2H\text{-}1B}$	J_{1HAB}
LCL150	3.4	3.5	11.2	4.3	7.3	11.3	2.3	5.1	8.5
LCL29		(—)[a]		4.2	6.5	11.4	2.1	3.8	11.5
LCL88	4.8	4.5	12.9		(—)[b]			(—)[c]	
LCL30	4.5	2.7	11.1		(—)[b]			(—)[c]	
LCL275	5.7	2.3	12.1	4.2	7.2	11.5	3.4	6.0	11.7
LCL277	5.8	2.4	12.1	4.2	6.9	11.2	4.1	6.6	11.1
C2-Cer	3.9	3.2	11.3	4.3	6.2	11.2		N/A	
C6-Cer	3.6	3.2	11.3		(—)[b]			N/A	
C12-Cer	3.6	3.1	11.3		(—)[b]			N/A	
C16-Cer	3.7	3.0	11.3		(—)[b]			N/A	

N/A, not available.

[a] Appeared as a two identical doublets with $J = 11.3$ Hz.

[b] Appeared as a one doublet with $J = 5.1$ Hz.

[c] Appeared as a one broad singlet with the half width ~7 Hz.

was not affected by a close proximity of the pyridinium ring. On the other hand, the NMR spectra of CCPS analogs in D_2O showed changes in the chemical shift (δ) values and multiplicity of the protons located in their polar head. This effect depended on the chain lengths and the locations of the PSU (Fig. 2C). The following order of downfield shift of 2-H and 3-H resonances was observed: **LCL30 < LCL88 < LCL29 < LCL277 < LCL150 < LCL275**. Moreover, this pattern follows the previously observed decreasing order of the R_M values of CCPS analogs, confirming a site-specific influence of the PSU on their polarity. Different deshielding trend was observed for the methylene protons 1-H_A and 1-H_B: **LCL29 < LCL277 < LCL150 < LCL30 < LCL88 < LCL275**. Similar pattern of changes was also recorded in CD_3OD solution. Significant separation of the resonance signals of the methylene 1-$H_{A,B}$ protons was observed for **LCL150**, **LCL277**, and **LCL275** ($\Delta\delta$ = .07–0.10 ppm), and a marginal for **LCL29** ($\Delta\delta$ = .04 ppm). Contrary to this, these protons remained magnetically equivalent in **LCL88** and **LCL30** (sharp one doublet with J = 5.1 Hz in CD_3OD or a broad singlet with the halfwidth ~7.0 Hz in D_2O, Table 2). Moreover, in the case of **LCL150**, **LCL277**, and **LCL275**, the observed shielding effect of the 2-H and 6-H protons $\Delta\delta \sim 0.05$ ppm) located in the pyridinium rings by the ligands situated in their polar heads confirms the presence of the mutual electronic effects.[91]

In conclusion, all D-*e*-ω-CCPS homologs, except C2-ω-CCPS, behaved similarly in D_2O and CD_3OD as their corresponding Cers in CD_3OD. When the PSU was located internally and in a close proximity to the polar head of Cer, its profound effect on the conformational preferences of the polar head of lipid was observed.

2.2. Cellular levels of CCPS analogs

Cellular levels of CCPS analogs were quantitated by LC–MS analysis. Experimental data from cell treatment with 5 μM concentrations of CCPS analogs over the indicated time showed a very fast cellular uptake for ω-CCPS homologs and their dhCCPS analogs (Fig. 3A and B). Intracellular level of these lipids after 15 min of treatment was established as 1–2% of the concentration applied (500–1000 pmol/1 × 10^6 cells) with a progressive increase over time, except for C16-and C12-dhCCPS analogs. When treatment time was extended to 24 h, differences in the cellular level of the short-chain and long-chain homologs were noticed. Levels of **LCL150** and **LCL29** continuously increased up to 21% and 15%, respectively, whereas C12 and C16-homologs showed a plateau (at 5 and 24 h treatments, respectively). Cellular levels of dihydro analogs were also time- and chain length-dependent. Levels of the short-chain homologs permanently increased to 7.5% and 11% at 5 h and 18% and 22% at 24 h (**LCL143** and **LCL319**, respectively), whereas the long-chain homologs reached a plateau at 1–2 h of the treatments.

Comparison between the cellular levels of the parallel pairs of ω-CCPS and ω-dhCCPS revealed that the long-chain ω-CCPSs were present at a higher level than

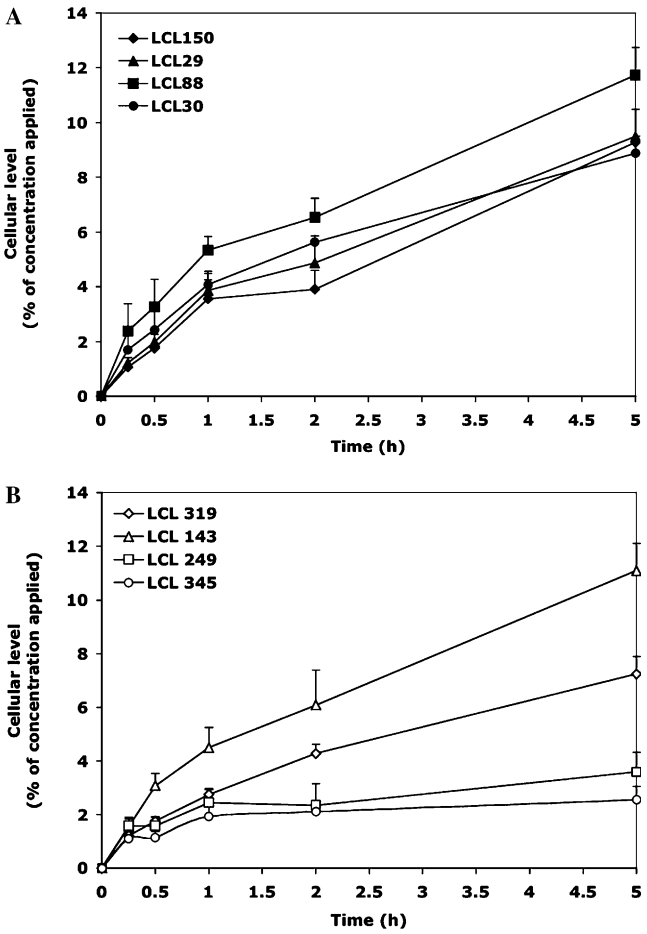

Figure 3. Cellular levels of D-*e*-ω-CCPS and D-*e*-ω-dhCCPS analogs. MCF7 cells were treated with 5 μM concentration of CCPS analogs over the indicated time, and cellular levels of the intact CCPSs were measured by the MS methodology as shown under Section 4. Results are expressed as % of concentration applied. These assays were performed using duplicate samples in two independent experiments. (A) Cellular levels of ω-CCPSs: **LCL150** (C2-ω-CCPS), **29** (C6-ω-CCPS), **88** (C12-ω-CCPS), and **30** (C16-ω-CCPS). (B). Cellular levels of ω-dhCCPSs: **LCL319** (C2-ω-dhCCPS), **143** (C6-ω-dhCCPS), **249** (C12-ω-dhCCPS), and **345** (C16-ω-dhCCPS).

their dihydro-counterparts: 8.5% versus 2.7% and 11.6% versus 3.2% for 5 h treatment (**LCL30/LCL345** and **LCL88/LCL249**, respectively). The level of D-*e*-C6-ω-dhCCPS was slightly higher than its corresponding D-*e*-C6-ω-CCPS, whereas levels of D-*e*-C2-ω-CCPS and D-*e*-C2-ω-dhCCPS were similar. Further investigation showed that this phenomenon was caused by the chain-specific metabolism of ω-dhCCPS to the corresponding ω-CCPS analogs.

2.3. Inhibitory effect of CCPS lipids on MCF7 cell growth

To examine the anticancer activity of the newly synthesized Cer analogs, we analyzed their inhibitory effect on MCF7 breast carcinoma cells (Fig. 4 and Table 3). As shown in Figure 4, all tested D-*e*-Cn-ω-CCPS homologs (C2–C16) showed inhibitory effects on cell growth with the following IC_{50} values (μM): 8.0/C2, 1.0/C6, 0.6/C12, and 1.6/C16. At 1.0 μM concentration the most effective was the C12-homolog (**LCL88**), and the least

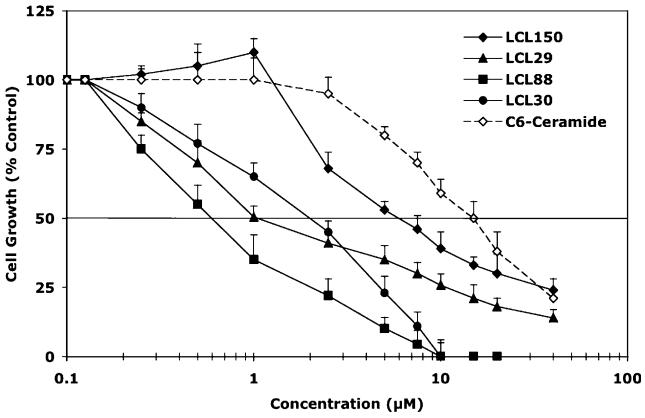

Figure 4. Dose-dependent inhibitory effects of D-*e*-C_n-ω-CCPS homologs and D-*e*-C6-Cer: **LCL150** (C2-ω-CCPS), **29** (C6-ω-CCPS), **88** (C12-ω-CCPS), and **30** (C16-ω-CCPS) on survival of MCF7 breast carcinoma cells after 4 8h treatment. Cell proliferation and cell viability were determined by Trypan blue exclusion assays. These assays were performed using duplicate samples in two or three independent experiments.

Table 3. IC_{50} values (μM) of ceramidoids determined from the dose-dependent experiments after 48 h treatments

Compound	Abbreviation code	Cytotoxicity
LCL150	D-*e*-C2-ω-CCPS	6.0
LCL29	D-*e*-C6-ω-CCPS	1.0
LCL124	L-*t*-C6-ω-CCPS	1.0
LCL187	L-*e*-C6-ω-CCPS	7.5
LCL272	D-*t*-C6-ω-CCPS	5.0
LCL88	D-*e*-C12-ω-CCPS	0.6
LCL30	D-*e*-C16-ω-CCPS	2.1
LCL87	L-*t*-C16-ω-CCPS	2.2
LCL255	L-*e*-C16-ω-CCPS	2.9
LCL319	D-*e*-C2-ω-dhCCPS	18.5
LCL143	D-*e*-C6-ω-dhCCPS	5.0
LCL249	D-*e*-C12-ω-dhCCPS	2.5
LCL345	D-*e*-C16-ω-dhCCPS	2.5
LCL186	D-*e*-C6-ω-DMAS-CCPS	4.4
LCL275	D-*e*-C1-α-CCPS	20.0
LCL277	D-*e*-C3-γ-CCPS	8.5
LCL23	D-*e*-C6-Cer	15.0

Cell proliferation and cell viability were determined by Trypan blue exclusion assays. These assays were performed using duplicate samples in two or three independent experiments.

potent was the C2-homolog (**LCL150**). Some inhibitory effect (20–30%) was already observed at 0.2 μM of the C12-, C6-, and C16-homologs. Additionally, the inhibitory effects of CCPS analogs were compared to the activity of D-*e*-C2-Cer and D-*e*-C6-Cer. These two synthetic Cers are commonly used in cell experiments as cell permeable homologs of naturally occurring long-chain Cers. C2-Cer was inactive up to a 20 μM concentration (data not shown), whereas C6-Cer showed only a low inhibitory effect with IC_{50} value corresponding to 15.0 μM at 48 h (Fig. 4).

We also noticed remarkable differences in the activity profile between the C6- and C16-homologs. D-*e*-C6 (**LCL30**) showed a systematic, dose-dependent inhibitory effect on cell growth from 0.2 to 10.0 μM, and at 5 μM it was more potent than **LCL29**. **LCL29** was very potent at concentrations 0.1–1.0 μM. When concentrations were increased up to 10 μM, we did not find any further significant changes. This observation may suggest a different mechanism of action for the short- and the long-chain Cers.[21]

The effects of D-*e*-ω-dhCCPS analogs on cell growth were also investigated. DhCers are believed to be biologically inactive compounds as was shown for C2- and C6-homologs.[8,11] However, D-*e*-C6-, C12-, and C16-ω-dhCCPS homologs (**LCL143**, **249**, and **345**) showed a concentration-dependent inhibitory effect on cell growth, although with a lower potency as compared to their 4–5 unsaturated counterparts (**LCL29**, **88**, and **30**). As shown in Table 3, the IC_{50} values (μM) for 48 h treatment were as follows: 2.5/**LCL345**, 2.5/**LCL249** and 5.0/**LCL143**. C2-homolog, **LCL319**, had a low activity and only 15% of inhibitory effect was observed for 10 μM treatment. The fluorescent C6-Cer analog, D-*e*-C6-DMAS-ω-CCPS (**LCL186**), also showed inhibitory effect on MCF7 cells growth ($IC_{50} \sim 4$ μM for 48 h treatment).

Stereospecific effect of CCPS analogs was studied for C6- and C16-ω-CCPS analogs (IC_{50} values are shown in Table 3). All tested stereoisomers of C6-ω-CCPS (**LCL29**, **124**, **187**, and **272**) caused inhibitory effects on MCF7 cell growth with the (2*S*)- isomers (**LCL29**, **124**) being more potent than their (2*R*)-isomers (**LCL187**, **272**). A similar stereo-specificity was observed for the parent C6-Cers in HL-60 cells (A. Bielawska, unpublished). (2*S*)-Isomers of C16-ω-CCPS (D-*e*: **LCL30** and L-*t*-: **LCL87**) showed a similar, concentration-dependent (1.0–10.0 μM) inhibitory effect on cell growth at 48 h and a time-dependent anti-proliferative effect for 1 μM treatment over a 0–72 h time period (not shown). Similarly, no significant difference in the activity of C16-ω-CCPS enantiomers (**LCL30** and **LCL255**) was noticed (not shown).

We tested also inhibitory effects of **LCL275** and **277** (D-*e*-C1-α- and D-*e*-C3-γ-CCPS analogs; IC_{50} values are shown in Table 3). Considering the length of the *N*-acyl-moiety of **LCL275** and **LCL277** they are C12- and C10-homolog mimics, and these compounds can be treated as close analogs of **LCL88**. However, the placement of the PSU in the α or γ positions to the carbonyl group allows comparison to **LCL150** (where the PSU is at the β-position to the carbonyl group). Neither **LCL275** nor **LCL277** followed the activity pattern of **LCL88**; rather their activity resembled that of **LCL150**. They showed inhibitory effects at a higher concentration (IC_{50} values are 8.5 μM/**LCL277** and 20 μM/**LCL275**). In summary, a close location of the PSU to the polar head of Cer structure decreased the potency of these analogs, with **LCL275** being the least potent compound from the CCPS family. On the other hand, CPB, a one-chain cationic surfactant, was not active compound as well and did not show any influence on the isolated mitochondria as CCPS analogs.[73,74] The above results correlate well with the NMR data and the hydrophobicity R_M values for these analogs (Figs. 1 and 2C). The close proximity of the PSU to the polar heads of **LCL150**, **275**, and **277** significantly altered their conformations and polarity level in comparison to Cer itself. These factors can be responsible for diminished

delivery and not efficient binding of these analogs by the prospective protein targets.

In conclusion, these results suggest that the long-chain ω-CCPS and ω-dhCCPS analogs (C12- and C16-homologs), which mimic the natural Cers, can serve as molecular tools to study actions and metabolism of the natural long-chain Cers and dhCers in vitro (vide infra).

2.4. Oxidation of ω-dhCCPS homologs to their corresponding ω-CCPS analogs in MCF7 cells

As mentioned above, ω-dhCCPS analogs showed a concentration-dependent inhibitory effect on cell growth, although with a lower potency as compared to their unsaturated analogs. Comparison of the cellular levels of ω-CCPS and ω-dhCCPS analogs for the same concentration treatment (Fig. 3A and B) indicated that ω-dhCCPS analogs are present at a much lower level, except for the C6-homolog. LC–MS analysis of lipid components from MCF7 cells treated with **LCL249** and **345** (dhC12 and dhC16 homologs) showed a time-dependent generation of D-*e*-C12- and C16-ω-CCPS (**LCL88** and **LCL30**) Figure 5A and B. **LCL249** was metabolized to **LCL88** very fast (15% of LCL88 was generated after 15 min treatment reaching 70% after 24 h). Desaturation of C16-homolog, **LCL345**, was delayed, and the appearance of LCL30 was detected only after 1 h treatment (~25%). Generation of **LCL30** from **LCL345** was also time-dependent and for 24 h treatment **LCL30** was a major component reaching 60% of total. Metabolic generation of active Cers from its inactive precursor dhCers may explain the inhibitory effect on cell growth observed after treatment with the long-chain analogs: **LCL 249** and **345**. Additionally, it may suggest that long-chain cationic dhCers are able to reach compartments where dihydro-Cer desaturase (dhCerD) is present. On the other hand, treatment with the C6-analog, **LCL143**, did not show any formation of its unsaturated analog, even for the extended time of the experiment. As discussed above, both C6-analogs, **LCL29** and **LCL143**, showed time-dependent increase of cellular levels (but with a higher value for **LCL143**) and caused inhibitory effects on cell growth, although with a much lower potency for **LCL143**. Our experiments using D-*e*-C6-dhCer build upon an unnatural 17C-sphingoid backbone (D-*e*-17C6-dhCer)[21] showed no formation of the corresponding 17C6-Cer (data not shown). Interestingly, the presence of the long-chain 17dhCers and a time-delayed formation of the corresponding 17Cers were observed. It is most likely that **LCL143** followed the same metabolic pattern as C6-dhCer, that is, formation of the long-chain Cers as a result of its N-deacylation following recycling of the formed sphingosine.[11,21] The increase of the endogenous Cers caused by **LCL143** is shown below (Fig. 6B).

2.5. Effects of CCPS analogs on endogenous Cers in MCF7 cells

Active agonists usually cause an increase of the endogenous Cers levels, followed by cell death.[4–9] This effect was also observed when cells were treated with exogenous C2- and C6-Cers at the appropriate concentrations.[1,11–13] To examine the effects of the CCPS analogs on the levels and composition of the endogenous Cers, we applied LC–MS technique, as described in Section 4. The effects of CCPS analogs on endogenous Cer are shown in Figure 6. Treatment with 5 μM of **LCL 29**, **30**, and **88** caused generation of endogenous Cer (Fig. 6A). A small increase in the total Cer was observed after 1 h of treatment for **LCL88** and **LCL30**, and was increased at 5 h to 180%, 135% and 130% for **LCL88**, **29**, and **30**, respectively. **LCL29** caused a time-dependent increase of Cer up to 24 h (~200%), whereas Cer level generated by **LCL30** and **LCL88** remained similar as observed for 5 h treatment. **LCL88** at concentration 1 μM showed a fast increase of Cer up to 5 h, and this level was almost unchanged (only ~10% increase) up to 48 h (not shown). The C2-homolog, **LCL150**, showed an inhibitory effect on endogenous Cer, decreasing its level to ~50% for 1 h treatment without recovery up to 24 h treatment. These results point to a different mechanism of action for C2-homolog on the metabolism of endogenous Cers. As shown in Figure

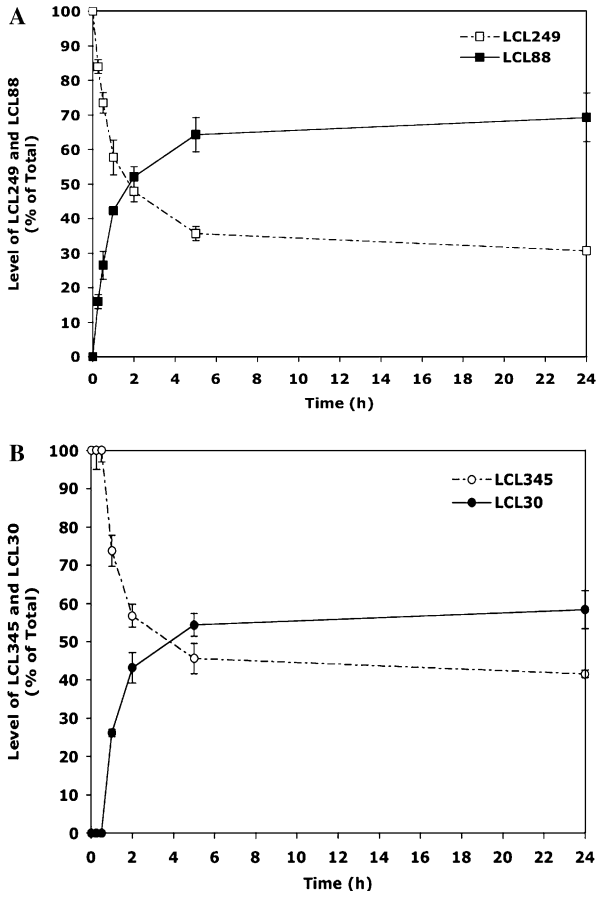

Figure 5. omega-DhCCPS analogs serve as substrates for dihydroceramide 4,5-desaturase in MCF7 cells to generate the corresponding ω-CCPS analogs. Absolute levels (pmol) of ω-dhCCPS and ω-CCPS analogs were determined by MS method as described under Section 4. Data are expressed as changes of the particular ω-dhCCPS and ω-CCPS to the total level of ω-dhCCPS and ω-CCPS (100%). (A) Time-dependent formation of D-*e*-C12-ω-CCPS from D-*e*-C12-ω-dhCCPS. (B) Time-dependent formation of D-*e*-C16-x-CCPS from D-*e*-C16-x-dhCCPS.

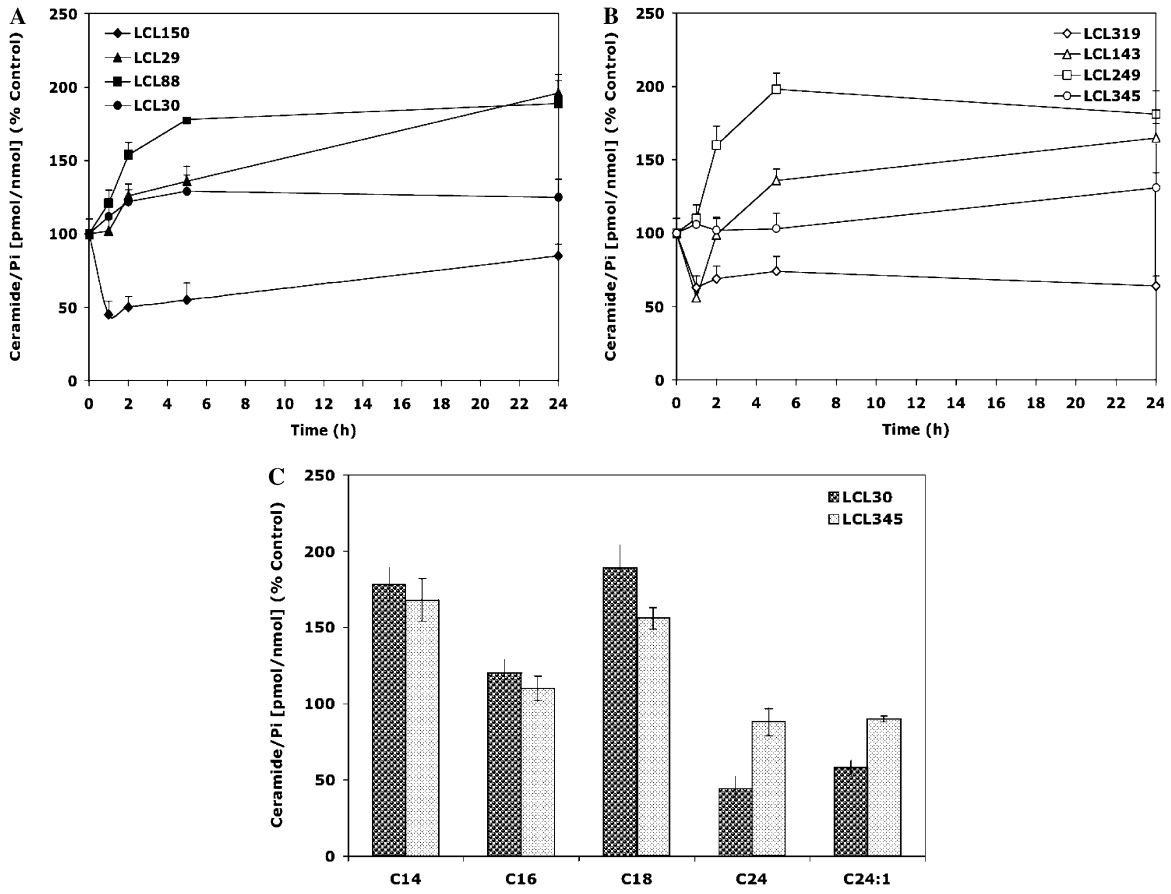

Figure 6. Effects of ω-CCPS and ω-dhCCPS on endogenous Cer. To examine the effects of newly synthesized ceramidoids on the level and composition of the endogenous Cer, we used LC–MS as described under Section 4. Data are expressed as changes in the total Cer level (pmol) or individual Cer components (pmol) normalized to the phospholipid phosphate (Pi) levels (nmol) present in the Bligh and Dyer lipid extract in relation to the control cells: Cer/Pi [pmol/nmol] (% control). (A) Time-dependent effects of 5 μM D-*e*-C2-C16-ω-CCPS homologs (**LCL29**, **30**, **88**, and **150**) on the total endogenous Cers. (B) Time-dependent effects of 5 μM D-*e*-C2-C16-ω-dhCCPS homologs (**LCL143**, **249**, **319**, and **345**) on the total endogenous Cers. (C) Effects of 5 μM D-*e*-C16-ω-CCPS (**LCL30**) and 5 μM D-*e*-C16-ω-dhCCPS (**LCL345**) on endogenous Cer species. Results shown for 1 h treatment.

6B, treatment with dh-CCPS analogs caused also changes in the level of endogenous Cers. A very fast increase was observed for the C12-homolog (**LCL249**, 160% for 1 h and 200% for 5 h treatment). However, the C16-homolog did not affect the endogenous Cer (only ~20% increase was noticed for 24 h treatment). The C6-homolog caused an early downregulatory effect on Cers, followed by fast recovery and later increase, but to a lower extent, as compared to the C12-homolog. D-*e*-C2-ω-dhCCPS (**LCL319**), similar to its saturated analog (**LCL150**), caused a permanent decrease in endogenous Cers.

CPPS analogs, except for **LCL150**, had a regulatory effect on the composition of endogenous Cers. C16-, C24-, and C24:1-Cers are the major components of the control cells (~90% of the total Cers). Treatment with **LCL30** caused changes of Cer species, increase of C16-, C14-, and C18-Cers and decrease of C24- and C24:1-Cers. At 1 h time point, the levels of the endogenous C16-, C14-, and C18-Cers were increased up to 120%, 170%, and 190%, respectively, whereas the endogenous C24:0- and C24:1-Cers decreased below the control level (44% and 60%, respectively) (Fig. 6C). Further increase of C14- and C18-Cers (320% and 353% at 5 h and 360% and 440% at 24 h) was observed, however without so significant further increase for C16-Cer. The decrease in C24-Cer was permanent, but the level of C24:1 Cer slowly recovered. **LCL88** and **LCL29** (C12- and C6-homologs) followed the pattern of **LCL30**, showing a time-dependent increase for C16-, C14-, and C18-Cers and decrease in C24- and C24:1-Cers. The most effective was the C12-homolog, which increased the levels of C16-, C14-, and C18-Cers up to 205%, 594%, and 385%, respectively, after 5 h treatment. The C2-homolog did not follow the above pattern and caused decreases in all Cer species (data not shown).

ω-DhCCPS homologs had also regulatory effects on endogenous Cers compositions, but with a lower extent as compared to their unsaturated analogs. As shown in Figure 6C, treatment with **LCL345** for 1 h increased already C14- and C18-Cers (170% and 160%). Small changes for C16-Cer (~10% increase) and C24- and C24:1-Cers (~15% decrease) were also noticed. The increases in C14- and C18-Cers were time-dependent, reaching 400% and 600%, respectively, for a 24 h treatment. A permanent decrease was observed for C24-Cer (~50% for 24 h). Again, the D-*e*-C12-ω-dhCCPS

(**LCL249**) was the most potent regulator in this group: the levels of C16-, C14-, and C18-Cers up to 125%, 305%, and 425% after 5 h treatment and 185%, 1300%, and 406% for the 24 h time point (data not shown).

These observations suggest that CCPS analogs can reach specific cell compartments very fast (level of cellular **LCL30** at 15 min was already ~400 pmol) and access specific enzymes of Cer metabolism as their early targets.

3. Conclusions

We have designed, synthesized, and characterized a series of Cer and dhCer conjugates with pyridinium salts (CCPS and dhCCPS) as model compounds to study properties of mitochondriotropic Cers under physiological conditions. The results obtained in this study corroborate the hypothesis that site-specific cationization of Cer exerts critical effects on the physicochemical and targeting properties with enhanced anticancer activity. CCPS and dhCCPS analogs, as expected, showed significantly improved solubility in water, leading to well-resolved NMR spectra in D_2O, broadly modified hydrophobicity, fast cellular uptake, and higher anticancer activities in comparison to uncharged counterparts.

Activity of the D-*e*-series of ω-CCPS analogs was chain length-dependent, the most potent were the C6- and C12-homologs, and the least potent were the C2-homologs. Moreover, the C6- and C12-homologs represented the most potent Cer-based anticancer agents reported so far. Modest stereochemical effects on cell growth were noticed, the 2*S*-isomers were more potent than their 2*R*-counterparts. DhCCPS analogs were also active but with a much lower potency than the unsaturated counterparts. Long-chain ω-dhCCPS analogs, once delivered to cells, were metabolized to the corresponding unsaturated ω-CPPS analogs. These compounds can be used as convenient substrates to study activity of dhCer desaturase enzyme by in vitro and in vivo experiments. D-*e*-C16-ω-CCPS caused early changes in endogenous Cer species (downregulation of C24- and C24:1-Cers, and upregulation of C14-, C16-, and C18-Cers).

Evaluation of physicochemical and biological properties of these novel ceramidoids indicated that either the short chain or the very long-chain analogs could have diminished capabilities to penetrate cell membranes and be efficiently delivered into cancer cells or tumor tissues. However, a better overall anticancer efficiency could be expected for moderately polar and very well water-soluble ceramidoids, considering their application in animal experiments.

4. Experimental

4.1. Chemistry

All solvents and general reagents were purchased from Aldrich. Stereoisomers of sphingosine (**1**–**4**) and D-*e*-4,5-dihydro-sphingosine (**5**) were prepared as described previously.[92–94] D-*e*-C2-C16-Cers were prepared by N-acylation of 1 using acetyl, hexanoyl, dodecanoyl or hexadecanoyl chlorides as reported.[8,57] Reaction progress was monitored by the analytical normal and reverse-phase thin layer chromatography (NP TLC or RP TLC) using aluminum sheets with 0.25 mm silica gel 60-F_{254} (Merck) and 0.150 mm C18-silica gel (Sorbent Technologies). Detection was done by the PMA reagent (ammonium heptamolybdate tetrahydrate cerium sulfate (5:2, g/g) in 125 mL of 10% H_2SO_4) and the Dragendorff reagent (Fluka) following heating of the TLC plates at 170 °C or by the UV (254 nm). Flash chromatography was performed using EM Silica Gel 60 (230–400 mesh) with the indicated eluent systems. Melting points were determined in open capillaries on Electrothermal IA 9200 melting point apparatus and are reported uncorrected. Optical rotation data were acquired using a Jasco P-1010 polarimeter. ^{1}H NMR spectra were recorded on Bruker AVANCE 500 MHz spectrometer equipped with Oxford Narrow Bore Magnet. Chemical shifts are reported in ppm on the δ scale from the internal standard of residual chloroform (*7.26* ppm). Mass spectral data were recorded in a positive ion electrospray ionization (ESI) mode on Thermo Finnigan TSQ 7000 triple quadrupole mass spectrometer. Samples were infused in methanol solution with an ESI voltage of 4.5 kV and capillary temperature of 200 °C.[21,95]

4.1.1. General procedure A for the preparation of ceramides 6-12. To a well-stirred mixture of sphingoid base (**1**–**5**, 0.67 mmol) in 50% aqueous solution of sodium acetate (5 mL) and THF (12 mL), ω-bromoacyl bromide or chloride (2 mmol) was added dropwise at room temperature. Reaction mixture was stirred for 20 min until a complete conversion to Cer was achieved (TLC). Organic phase was separated and the aqueous layer was extracted twice with ethyl acetate (2× 10 mL). The combined organic phases were dried over anhydrous magnesium sulfate and evaporated under a reduced pressure to dryness to give a crude product. This material was purified by flash chromatography (elution with $CHCl_3$–MeOH–concd NH_4OH, 5:1:0.05, v/v/v) following crystallization.

4.1.1.1. D-*erythro*-2-*N*-(2′-Bromoacetyl)-sphingosine (6). Prepared from **1**. Pure product was obtained in 73% yield after crystallization from ethyl acetate as white microcrystalline powder, mp 79–81 °C; TLC ($CHCl_3$/MeOH, 5:1, v/v), R_f 0.52; $[\alpha]_D^{22}$ +6.0° (c = 1, $CHCl_3$); $[\alpha]_{365}^{22} = +17.4°$ (c 1, $CHCl_3$); ^{1}H NMR (500 MHz, $CDCl_3$) δ 7.19 (d, 1H, J = 7.8, NH), 5.81 (dtd, 1H, J = 15.5, 6.8, 1.1, 5-H), 5.52 (ddt, 1H, J = 15.5, 6.8, 1.1, 4-H), 4.35 (t, 1H, J = 5.1, 3-H), 4.02 (dd, 1H, J = 11.4, 3.4, 1-H_A), 3.9 (d, 2H, J = 2.4, CH_2Br), 3.88 (m, 1H, 2-H), 3.73 (dd, J = 11.4, 3.5, 1-H_B), 2.06 (q, 2H, J = 7.1, C(6)H_2), 1.36 (m, 2H, C(7)H_2), 1.24 (m, 20H, CH_2), 0.87 (t, 3H, J = 7.1, CH_3); ESI-MS (CH_3OH, relative intensity, (%) *m*/*z* 864.8, 862.7, and 860.8 ($[2M+Na]^+$, 50, 100 and 60), 442.1 and 444.1 ($[M+Na]^+$, 4 and 4), 419.7 and 421.7 (MH^+, 3 and 3), 402.0 and 404.0 ($[MH-H_2O]^+$, 21

and 20), 264.2 (3). Calcd for $C_{20}H_{38}{}^{79}BrNO_3$ *m/z* 419.2; Calcd for $C_{20}H_{38}{}^{81}BrNO_3$ *m/z* 421.2; Anal. Calcd for $C_{20}H_{38}BrNO_3$ (420.40): C, 57.14; H, 9.11; N, 3.33; Br, 19.01. Found: C, 57.24; H, 9.19; N, 3.30; Br, 18.97.

4.1.1.2. D-*erythro*-2-*N*-(2′-Bromoacetyl)-4,5-dihydrosphingosine (7). Prepared from **5**. Pure product was obtained in 65% yield after crystallization from *n*-hexane–acetone (3:1, v/v) as a white microcrystalline powder, mp 129–131 °C; TLC ($CHCl_3$/MeOH, 5:1, v/v) R_f 0.54; $[\alpha]_D^{25}$ +5.60° (*c* 1, MeOH); $[\alpha]_{365}^{25}$ +11.20° (*c* 1, MeOH)[1] H NMR (500 MHz, $CD_3OD/CDCl_3$, 1:10, v/v) δ 3.86 (dd, 1H, J = 11.5, 3.7, 1-Ha), 3.70 (m, 1H, 2-H), 3.63 (m, 2H, 3-H, and 1-Hb), 3.07 (s, 2H, CH_2Br), 1.45 (m, 4H, C(4)H_2 and C(5)H_2), 1.18 (m, 24H, CH_2), 0.81 (t, 3H, J = 7.1, CH_3); ESI-MS (CH_3OH, relative intensity, %) *m/z* 868.7, 866.8, and 864.7 ($[2M+Na]^+$, 45, 100, and 60), 446.3 and 444.5 ($[M+Na]^+$, 8 and 9), 423.7 and 421.9 (MH^+, 11 and 13), 406.0 and 404.0 ($[MH-H_2O]^+$, 5 and 4). Calcd for $C_{20}H_{40}{}^{79}BrNO_3$ *m/z* 421.2; Calcd for $C_{20}H_{40}{}^{81}BrNO_3$ *m/z* 423.2; Anal. Calcd for $C_{20}H_{40}BrNO_3$ (422.4): C, 56.86; H, 9.54; N, 3.32; Br, 18.91. Found: C, 57.04; H, 9.58; N, 3.31; Br, 18.89.

4.1.1.3. D-*erythro*-2-*N*-(6′-Bromohexanoyl)-sphingosine (8). Prepared from **1**. Pure product was obtained in 79% yield after crystallization from *n*-hexane–ethyl acetate (4:1, v/v) a as white microcrystalline powder, mp 48–50 °C; TLC ($CHCl_3$/MeOH, 5:1, v/v) R_f 0.60; $[\alpha]_D^{22}$ −2.95° (*c* 1, $CHCl_3$) and −10.3° (*c* 1, MeOH); $[\alpha]_{365}^{22}$ −16.2° (*c* 1, $CHCl_3$) and −35.1° (*c* 1, MeOH); ^{1}H NMR (500 MHz, $CDCl_3$) δ 6.28 (d, 1H, J = 7.4, NH), 5.78 (dt, 1H, J = 15.4, 6.8, 5-H), 5.52 (dd, 1H, J = 15.4, 6.4, 4-H), 4.31 (t, 1H, J = 4.8, 3-H), 3.95 (dd, 1H, J = 11.3, 3.6, 1-Ha), 3.90 (m, 1H, 2-H), 3.69 (dd, J = 11.3, 3.3, 1-Hb), 3.40 (t, 2H, J = 6.8, C(6′)H_2Br), 2.24 (t, 2H, J = 7.5, $COCH_2$), 2.04 (q, 2H, J = 7.1, C(6)H_2), 1.88 (m, 2H, C(5′) H_2C(6′)H_2Br), 1.66 (m, 2H, $COCH_2CH_2$), 1.48 (m, 2H, CO $CH_2CH_2CH_2$), 1.35(m, 2H, C(7)H_2), 1.25 (m, 20H, CH_2), 0.87 (t, 3H, J = 7.0, CH_3); ESI-MS (CH_3OH, relative intensity, %) *m/z* 976.9, 974.9, and 972.8 ($[2M+Na]^+$, 60, 100, and 85), 477.8 and 475.8 (MH^+, 21 and 23), 460.0 and 458.0 ($[MH-H_2O]^+$, 14 and 17), 264.2 (3). Calcd for $C_{24}H_{46}{}^{79}BrNO_3$ *m/z* 475.3; Calcd for $C_{24}H_{46}{}^{81}BrNO_3$ *m/z* 477.3; Anal. Calcd for $C_{24}H_{46}BrNO_3$ (476.5): C, 60.49; H, 9.73; N, 2.94; Br, 16.77. Found: C, 60.22; H, 9.73; N, 2.96; Br, 16.88.

4.1.1.4. L-*threo*-2-*N*-(6′-Bromohexanoyl)-sphingosine (9). Prepared from **2**. Pure product was obtained in 70% yield after crystallization from *n*-hexane/ethyl acetate (8:1, v/v) as a white microcrystalline powder, mp 71–73 °C (wet at 64 °C); TLC ($CHCl_3$–MeOH, 5:1, v/v) R_f 0.59; $[\alpha]_D^{22}$ −2.30° (*c* 1, $CHCl_3$) and −19.0° (*c* 1, MeOH); $[\alpha]_{365}^{22}$ −15.3° (*c* 1, $CHCl_3$) and −71.0° (*c* 1, MeOH); ^{1}H NMR (500 MHz, $CDCl_3$) δ 6.10 (d, 1H, J = 7.4, NH), 5.73 (dt, 1H, J = 15.4, 6.7, 5-H), 5.45 (dd, 1H, J = 15.4, 6.5, 4-H), 4.37 (dd, 1H, J = 6.1 and 4.5, 3-H), 3.91 (m, 1H, 2-H), 3.80 (m, 2H, 1-Ha and 1-Hb), 3.40 (t, 2H, J = 6.8, C(6′)H_2Br), 2.52 (br s, 2H, OH), 2.23 (t, 2H, J = 7.5, $COCH_2$), 2.04 (q, 2H, J 6.9, C(6)H_2), 1.87 (m, 2H, C(5′)H_2C(6′)H_2 Br), 1.67 (m, 2H, $COCH_2CH_2$), 1.48 (m, 2H, CO $CH_2CH_2CH_2$), 1.33 (m, 2H, C(7)H_2), 1.24 (m, 20H, CH_2), 0.87 (t, 3H, J = 7.1, CH_3); ESI-MS (CH_3OH, relative intensity, %) *m/z* 977.2, 975.1, and 973.2 ($[2M+Na]^+$, 45, 100, and 71), 477.6 and 475.6 (MH^+, 19 and 21), 460.1 and 458.1 ($[MH-H_2O]^+$, 16 and 19), 264.2 (4). Calcd for $C_{24}H_{46}{}^{79}BrNO_3$ *m/z* 475.3; Calcd for $C_{24}H_{46}{}^{81}BrNO_3$ *m/z* 477.3; Anal. Calcd for $C_{24}H_{46}BrNO_3$ (476.5): C, 60.49; H, 9.73; N, 2.94; Br, 16.77. Found: C, 60.31; H, 9.68; N, 2.91; Br, 17.09.

4.1.1.5. L-*erythro*-2-*N*-(6′-Bromohexanoyl)-sphingosine (10). Prepared from **3**. Pure product was obtained in 71% yield after crystallization from *n*-hexane–ethyl acetate (4:1, v/v) as a white powder; $[\alpha]_D^{22}$ +2.75° (*c* 1, $CHCl_3$) and +9.90° (*c* 1, MeOH); $[\alpha]_{365}^{22}$ +16.8° (*c* 1, $CHCl_3$) and +36.1° (*c* 1, MeOH). Remaining data are identical as reported for **8**. Anal. Calcd for $C_{24}H_{46}BrNO_3$ (476.5): C, 60.49; H, 9.73; N, 2.94; Br, 16.77. Found: C, 60.10; H, 9.42; N, 2.81; Br, 16.71.

4.1.1.6. D-*threo*-2-*N*-(6′-Bromohexanoyl)-sphingosine (11). Prepared from **4**. Pure product was obtained in 64% yield after crystallization from *n*-hexane–ethyl acetate (6:1, v/v) as a white powder; $[\alpha]_D^{22}$ +2.15° (*c* 1, $CHCl_3$) and +20.0° (*c* 1, MeOH); $[\alpha]_{365}^{22}$ +14.2° (*c* 1, $CHCl_3$) and +75.0° (*c* 1, MeOH). Remaining data are identical as reported for **9**. Anal. Calcd for $C_{24}H_{46}BrNO_3$ (476.5): C, 60.49; H, 9.73; N, 2.94; Br, 16.77. Found: C, 60.21; H, 9.66; N, 2.82; Br, 16.63.

4.1.1.7. D-*erythro*-2-*N*-(6′-Bromohexanoyl)-4,5-dihydro-sphingosine (12). Prepared from **1e**. Pure product was obtained in 69% yield after crystallization from *n*-hexane–ethyl acetate (4:1, v/v) as a white microcrystalline powder, mp 101–103 °C, TLC ($CHCl_3$–MeOH, 5:1, v/v) R_f 0.62; $[\alpha]_D^{22}$ +4.08° (*c* 1, MeOH); $[\alpha]_{365}^{25}$ +5.63° (*c* 1, MeOH) ^{1}H NMR (500 MHz, CD_3OD–$CDCl_3$, 1:10, v/v) δ 3.90 (dd, 1H, J = 11.4, 3.7, 1-Ha), 3.72 (m, 1H, 2-H), 3.60 (m, 2H, 3-H and 1-Hb), 3.43 (t, 2H, J = 6.8, C(6′)H_2Br), 2.20 (t, 2H, J = 7.5, $COCH_2$), 2.01 (p, 2H, J = 7.5, C(5′)H_2C(6′)H_2 Br), 1.85 (m, 2H, $COCH_2CH_2$), 1.68 (m, 2H, C(4)H_2), 1.46 (m, 2H, CO $CH_2CH_2CH_2$), 1.20 (m, 24H, CH_2), 0.80 (t, 3H, J = 7.1, CH_3); ESI-MS (CH_3OH, relative intensity, %) *m/z* 980.8, 978.9, and 976.9 ($[2M+Na]^+$, 55, 100, and 50), 502.1 and 498.1 ($[M+Na]^+$, 12 and 11), 480.1 and 478.1 (MH^+, 36 and 43), 462.1 and 460.1 ($[MH-H_2O]^+$, 4 and 4). Calcd. for $C_{24}H_{48}{}^{79}BrNO_3$ *m/z* 477.3; Calcd for $C_{24}H_{48}{}^{81}BrNO_3$ *m/z* 479.3; Anal. Calcd for $C_{24}H_{48}BrNO_3$ (478.5): C, 60.24; H, 10.11; N, 2.93; Br, 16.70. Found: C, 59.93; H, 10.11; N, 2.90; Br, 16.91.

4.1.1.8. General procedure B for the preparation of ceramides 13–18. (A) Synthesis of 12-bromododecanoyl and 16-bromohexadecanoyl chlorides. 12-Bromododecanoic or 16-bromohexadecanoic acid (97%, 1.1 mmol) was dissolved in dry cyclohexane (4 mL) by stirring at 45 °C for 20 min. To this well-stirred and water-cooled mixture one drop (~0.02 mL) of dry

pyridine was added following oxalyl chloride (99%, 0.145 mL, 1.65 mmol) over 1 min. After the addition was completed, cooling bath was removed and the reaction mixture was heated at 50 °C for 15 min and then left to reach room temperature for an additional 30 min. The reaction mixture was evaporated to dryness by purging dry nitrogen gas into the reaction flask following drying under the vacuum (~1 torr) at +4 °C over 30 min. The freshly prepared acid chlorides were dissolved in dry THF and taken up directly to the next step.

(B) Synthesis of ceramides **13**–**18**. To a well-stirred mixture of sphingoid bases (**1**–**5**, 0.67 mmol) in 50% aqueous solution of sodium acetate (5 mL) and THF (10 mL), solution of 12-bromododecanoyl (0.326 mg) or 16-bromohexadecanoyl chloride (0.380 mg) in dry THF (3.0 mL) was added dropwise over 1 min. After the addition was completed, the reaction mixtures were stirred for an additional 20 min at room temperature. The organic layers were separated and the aqueous phases were extracted with ethyl acetate (3× 5 mL). The combined organic extracts were dried ($MgSO_4$), filtered, and evaporated to dryness under reduced pressure to give crude products. These ceramides were purified by flash chromatography following crystallization.

4.1.1.9. D-*erythro*-2-*N*-(12′-Bromododecanoyl)-sphingosine (13). Prepared from **1**. Crude product was purified by chromatography ($CHCl_3$–MeOH–concd NH_4OH, 10:2:0.5, v/v/v) following crystallization from *n*-hexane–ethyl acetate (5:1, v/v) to give pure **13** in 73% yield as a white microcrystalline powder, mp 71–73 °C; TLC R_f ($CHCl_3$–MeOH, 5:1, v/v) R_f 0.65; $[\alpha]_D^{22}$ −2.0° (*c* 1, $CHCl_3$) and −15.6° (*c* 1, MeOH); $[\alpha]_{365}^{22}$ −12.5° (*c* 1, $CHCl_3$) and −50.1° (*c* 1, MeOH); ^{1}H NMR (500 MHz, $CDCl_3$) δ 6.23 (d, 1H, J = 7.4, NH), 5.78 (dt, 1H, J = 15.4, 6.6, 5-H), 5.52 (dd, 1H, J = 15.4, 6.5, 4-H), 4.31 (t, 1H, J = 4.6, 3-H), 3.95 (dd, 1H, J = 11.2, 3.7, 1-Ha), 3.90 (m, 1H, 2-H), 3.69 (dd, 1H, J = 11.2, 3.7, 1-Hb), 3.39 (t, 2H, J = 6.8, C(12′)H_2Br), 2.22 (t, 2H, J = 7.5, $COCH_2$), 2.04 (q, 2H, J = 7.1, C(6)H_2), 1.84 (m, 2H, C(11′)H_2C(12′)H_2Br), 1.63 (m, 2H, $COCH_2CH_2$), 1.40 (m, 2H, C(10′)H_2C(11′)H_2C(12′)H_2Br), 1.35 (m, 2H, C(7)H_2), 1.25 (m, 32H, CH_2), 0.87 (t, 3H, J = 7.0, CH_3); ESI-MS (CH_3OH, relative intensity, %) *m*/*z* 1145.0, 1142.9, and 1141.9 ([2M+Na], 54, 100, 55), 1122.7, 1120.7, and 1118.4 ($[2M+H]^+$, 30, 96, 34), 584.2 and 582.2 ([M+Na], 10 and 8), 561.9 and 559.9 (MH^+, 50 and 58), 543.8 and 541.9 ($[MH-H_2O]^+$, 17 and 19). Calcd for $C_{30}H_{58}{}^{79}BrNO_3$ *m*/*z* 559.4; Calcd for $C_{30}H_{58}{}^{81}BrNO_3$ *m*/*z* 561.4; Anal. Calcd. for $C_{30}H_{58}BrNO_3$ (560.7): C, 64.26; H, 10.43; N, 2.50; Br, 14.25. Found: C, 64.06; H, 10.45; N, 2.51; Br, 14.54.

4.1.1.10. D-*erythro*-2-*N*-(12′-Bromododecanoyl)-4,5-dihydro-sphingosine (14). Prepared from **5**. Crude product was purified by chromatography ($CHCl_3$–MeOH–concd NH_4OH, 10:2:0.5, v/v/v) following crystallization from *n*-hexane–ethyl acetate (5:1, v/v) to give pure **14** in 71% yield as a white microcrystalline powder, mp 97–98 °C; TLC R_f ($CHCl_3$/MeOH, 5:1, v/v) R_f 0.67; $[\alpha]_D^{21}$ +5.9° (*c* 1, $CHCl_3$) and +3.1° (*c* 1, MeOH); $[\alpha]_{365}^{21}$ +14.5° (*c* 1, $CHCl_3$) and +5.5° (*c* 1, MeOH); ^{1}H NMR (500 MHz, $CDCl_3$) δ 6.35 (d, 1H, J = 7.7, NH), 4.01 (dd, 1H, J = 11.3, 3.5, 1-Ha), 3.83 (m, 1H, 2-H), 3.78 (m, 1H, 3-H), 3.75 (dd, 1H, J = 11.3, 3.5, 1-Hb), 3.41 (t, 2H, J = 6.9, C(12′)H_2Br), 2.65 (br s, 2H, OH) 2.23 (t, 2H, J = 7.5, $COCH_2$), 1.85 (p, 2H, J = 7.7, C(11′) H_2C(12′)H_2Br), 1.65 (m, 2H, $COCH_2CH_2$), 1.54 (m, 2H, C(4)H_2), 1.42 (m, 2H, C(10′) H_2C(11′)H_2C(12′)H_2Br), 1.25 (m, 36H, CH_2), 0.88 (t, 3H, J = 7.1, CH_3); ESI-MS (CH_3OH, relative intensity, %) *m*/*z* 1149.9, 1147.8, 1146.8, and 1144.8 ([2M+Na], 25, 65, 100, 50), 1126.7, 1125.7 and 1123.7 ($[2M+H]^+$, 22, 20, 4). Calcd for $C_{30}H_{60}{}^{79}BrNO_3$ *m*/*z* 561.4; Calcd for $C_{30}H_{60}{}^{81}BrNO_3$ *m*/*z* 563.4; Anal. Calcd for $C_{30}H_{60}BrNO_3$ (562.7): C, 64.03; H, 10.75; N, 2.49; Br, 14.20. Found: C, 63.79; H, 10.92; N, 2.54; Br, 14.44.

4.1.1.11. D-*erythro*-2-*N*-(16′-Bromohexadecanoyl)-sphingosine (15). Prepared from **1**. Crude product was purified by chromatography ($CHCl_3$–MeOH–concd NH_4OH, 8:1:0.05, v/v/v) following crystallization from *n*-hexane–ethyl acetate (1:2, v/v) to give pure **15** in 96% yield as a white microcrystalline powder, mp 87–89 °C; TLC R_f ($CHCl_3$–MeOH, 8: 1, v/v) R_f 0.65; $[\alpha]_D^{22}$ −3.1° (*c* 1, $CHCl_3$) and −12.3° (*c* 1, MeOH); $[\alpha]_{365}^{22}$ −14.2° (*c* 1, $CHCl_3$) and −46.4° (*c* 1, MeOH); ^{1}H NMR (500 MHz, $CDCl_3$) δ 6.22 (d, 1H, J = 7.5, NH), 5.77 (dt, 1H, J = 15.4, 6.8, 5-H), 5.52 (dd, 1H, J = 15.4, 6.8, 4-H), 4.31(t, 1H, J = 4.7, 3-H), 3.95 (dd, 1H, J = 11.2, 3.8, 1-Ha), 3.90 (m, 1H, 2-H), 3.70 (dd, J = 11.2, 3.3, 1-Hb), 3.40 (t, 2H, J = 6.8, C(16′)H_2Br), 2.22 (t, 2H, J = 7.5, $COCH_2$), 2.04 (q, 2H, J = 7.1, C(6)H_2), 1.84 (m, 2H, C(15′)H_2C(16′)H_2Br), 1.63 (m, 2H, $COCH_2CH_2$), 1.40 (m, 2H, C(14′)H_2C(15′)H_2C(16′)H_2Br), 1.35 (m, 2H, C(7)H_2), 1.25 (m, 40H, CH_2), 0.87 (t, 3H, J = 7.1, CH_3); ESI-MS (CH_3OH, relative intensity, %) *m*/*z* 1235.7, 1233.8, 1232.8 and 1230.7 ($[2M+H]^+$ 38, 86, 100, and 65), 618.0 and 616.0 (MH^+, 76 and 78), 600.2 and 598.2 ($[MH-H_2O]^+$, 17 and 19). Calcd for $C_{34}H_{66}{}^{79}BrNO_3$ *m*/*z* 615.4; Calcd for $C_{34}H_{66}{}^{81}BrNO_3$ *m*/*z* 617.4; Anal. Calcd for $C_{34}H_{66}BrNO_3$ (616.8): C, 66.21; H, 10.79; N, 2.27; Br, 12.95. Found: C, 66.09; H, 10.78; N, 2.32; Br, 12.74.

4.1.1.12. D-*erythro*-2-*N*-(16′-Bromohexadecanoyl)-4,5-dihydrosphingosine (16). Prepared from **5** as shown for **15** in 78% yield. Analytical sample was obtained by crystallization from *n*-hexane–ethyl acetate (1:3, v/v) as a white microcrystalline powder, mp 93–95 °C; TLC R_f ($CHCl_3$–MeOH, 8:1, v/v) R_f 0.67; $[\alpha]_D^{22}$ +4.94° (*c* 1, $CHCl_3$); $[\alpha]_{365}^{22}$ +12.6° (*c* 1, $CHCl_3$); ^{1}H NMR (500 MHz, $CDCl_3$) δ 6.25 (d, 1H, J = 7.6, NH), 3.95 (dd, 1H, J = 11.3, 3.4, 1-Ha), 3.77 (m, 1H, 2-H), 3.72 (m, 1H, 3-H), 3.69 (dd, 1H, J = 11.3, 3.4, 1-Hb), 3.34 (t, 2H, J = 6.9, C(16′)H_2Br), 2.16 (t, 2H, J = 7.5, $COCH_2$), 1.77 (p, 2H, J = 7.0, C(15′)H_2C(16′)H_2Br), 1.59 (m, 2H, $COCH_2CH_2$), 1.45 (m, 2H, C(4)H_2), 1.35 (m, 2H, C(14′)H_2C(15′)H_2C(16′) H_2Br), 1.19 (m, 36H, CH_2), 0.81 (t, 3H, J = 7.0, CH_3); ESI-MS (CH_3OH, relative intensity, %) *m*/*z* 1240.2, 1238.3, 1237.3, and 1235.3 ($[2M+H]^+$, 30, 62, 97, and 40), 621.5.0 and 618.4 (MH^+, 28 and 100), 602.5 and 600.5 ($[MH-H_2O]^+$, 7 and 8). Calcd for $C_{34}H_{68}{}^{79}BrNO_3$ *m*/*z* 617.4; Calcd for $C_{34}H_{68}{}^{81}BrNO_3$ *m*/*z* 619.4; Anal. Calcd for $C_{34}H_{68}BrNO_3$

(618.8): C, 65.99; H, 11.08; N, 2.26; Br, 12.91. Found: C, 65.63; H, 10.88; N, 2.19; Br, 12.86.

4.1.1.13. L-*threo*-2-*N*-(16′-Bromohexadecanoyl)-sphingosine (17). Prepared from **2** as shown for **15** in 82% yield. Analytical sample was obtained by crystallization from *n*-hexane–ethyl acetate (1:2, v/v) as a white microcrystalline powder, mp 98–100 °C; TLC R_f ($CHCl_3$/MeOH, 8: 1, v/v) R_f 0.66; $[\alpha]_D^{22}$ −2.70° (*c* 1, $CHCl_3$); $[\alpha]_{365}^{22}$ −16.0° (*c* 1, $CHCl_3$); ^{1}H NMR (500 MHz, $CDCl_3$) δ 6.09 (d, 1H, *J* = 7.7, NH), 5.73 (dtd, 1H, *J* = 15.4, 6.7, 1.0, 5-H), 5.45 (ddt, 1H, *J* = 15.4, 6.7, 1.0, 4-H), 4.38 (dd, 1H, *J* = 6.3 and 3.5, 3-H), 3.90 (m, 1H, 2-H), 3.80 (m, 2H, 1-Ha and1-Hb), 3.39 (t, 2H, *J* = 6.8, C(16′)H_2Br), 2.21 (t, 2H, *J* = 7.3, COCH_2), 2.02 (q, 2H, *J* = 7.0, C(6)H_2), 1.85(m, 2H, C(15′)H_2C(16′)H_2Br), 1.61 (m, 2H, COCH_2CH_2), 1.42 (m, 2H, C(14′)H_2C(15′)H_2C(16′)H_2Br), 1.24 (m, 20H, CH_2), 0.87 (t, 3H, *J* = 7.1, CH_3); ESI-MS (CH_3OH, relative intensity, %) *m*/*z* 1235.3, 1233.3, 1232.5 and 1230.5 ($[2M+H]^+$ 67, 100, 61, and 18), 618.4 and 616.4 (MH^+, 54 and 56), 600.5 and 598.5 ($[MH-H_2O]^+$, 35 and 33). Calcd for $C_{34}H_{66}{}^{79}BrNO_3$ *m*/*z* 615.4; Calcd for $C_{34}H_{66}{}^{81}BrNO_3$ *m*/*z* 617.4; Anal. Calcd for $C_{34}H_{66}BrNO_3$ (616.8): C, 66.21; H, 10.79; N, 2.2; Br, 12.95. Found: C, 66.13; H, 10.83; N, 2.32; Br, 12.81.

4.1.1.14. L-*erythro*-2-*N*-(16′-Bromohexadecanoyl)-sphingosine (18). Prepared from **3**. Pure product was obtained in 78% yield after crystallization from *n*-hexane–ethyl acetate (1:2, v/v) as a white powder; $[\alpha]_D^{22}$ +11.8° (*c* 1, MeOH); $[\alpha]_{365}^{22}$ +45.0° (*c* 1, MeOH); Remaining data are identical as reported for **15**. Anal. Calcd for $C_{34}H_{66}BrNO_3$ (616.8): C, 66.21; H, 10.79; N, 2.27; Br, 12.95. Found: C, 66.02; H, 10.64; N, 2.12; Br, 12.72.

4.1.1.15. D-*erythro*-2-*N*-Nicotinoyl-sphingosine (19). Prepared from **1** (200 mg, 0.67 mmol) and nicotinoyl chloride hydrochloride (97%, 245 mg, 1.34 mmol) according to the *Procedure A*. The crude product was purified by flash chromatography (elution with $CHCl_3$–MeOH–concd NH_4OH, 5:1:0.05, v/v/v) following crystallization from *n*-hexane–ethyl acetate (2:1) to give 195 mg (72%) of pure **19** as a white microcrystalline powder, mp 104–106 °C; TLC R_f ($CHCl_3$–MeOH, 8:1, v/v) R_f 0.17; ^{1}H NMR (500 MHz, $CDCl_3$) δ 9.01 (d, 1H, *J* = 2.0, 2-H_{Py}), 8.70 (dd, 1H, *J* = 1.6 and 4.8, 6-H_{Py}), 8.11 (dt, 1H, *J* = 2.0 and 7.9, 4-H_{Py}), 7.37 (dd, 1H, *J* = 4.8 and 7.9, 5-H_{Py}), 7.12 (d, 1H, *J* = 7.2, NH), 5.84 (dtd, 1H, *J* = 15.4, 6.7, 1.1, 5-H), 5.60 (ddt, 1H, *J* = 15.4, 6.7, 1.1, 4-H), 4.48 (t, 1H, *J* = 4.8, 3-H), 4.12 (m, 2H, 1-Ha and 2-H), 3.83 (dd, *J* = 4.0 and 12.1, 1-Hb), 2.05 (q, 2H, *J* = 7.1, C(6)H_2), 1.36 (m, 2H, C(7)H_2), 1.24 (m, 20H, CH_2), 0.87 (t, 3H, *J* = 7.1, CH_3); ESI-MS (CH_3OH, relative intensity, %) *m*/*z* 830.9 ($[2M+Na]^+$, 100), 405.2 (MH^+, 3 and 3). Calcd for $C_{24}H_{40}N_2O$ *m*/*z* 404.3. Anal. Calcd for $C_{24}H_{40}N_2O_3$ (404.6): C, 71.25; H, 9.97; N, 6.92. Found: C, 68.90; H, 9.85; N, 6.71.

4.1.1.16. D-*erythro*-2-*N*-[3′-(3″-Pyridyl)-propionoyl]-sphingosine (20). Prepared from **1** (200 mg, 0.67 mmol) and 3-pyridinopropionic acid (97%, 288 mg, 1.1 mmol) according to the *Procedure B*. The crude product was purified by flash chromatography ($CHCl_3$–MeOH–concd NH_4OH, 65:10:1, v/v/v) to give pure **20** (240 mg, 64%) as a white solid. Analytical sample of **20** was obtained by crystallization from *n*-hexane–ethyl acetate (5:1, v/v) to give white microcrystalline powder, mp 83–84.5 °C; TLC R_f ($CHCl_3$–MeOH, 8:1, v/v) R_f 0.18; ^{1}H NMR (500 MHz, $CDCl_3$) δ 8.44 (d, 1H, *J* = 1.5, 2-H_{Py}), 8.40(dd, 1H, *J* = 1.5 and 4.2, 6-H_{Py}), 7.45 (d, 1H, *J* = 7.7, 4-H_{Py}), 7.37 (dd, 1H, *J* = 10.3 and 15.1, 5-H_{Py}), 6.36 (d, 1H, *J* = 7.8, NH), 5.76 (dtd, 1H, *J* = 15.4, 6.7, 1.1, 5-H), 5.48 (ddt, 1H, *J* = 15.4, 6.2, 1.1, 4-H), 4.24 (t, 1H, *J* = 4.5, 3-H), 3.91 (dd, 1H, *J* = 3.5 and 11.4, 1-Ha), 3.85 (m, 1H, 2-H), 3.63 (dd, 1H, *J* = 3.4 and 11.4, 1-Hb), 2.97 (t, 2H, *J* = 7.4, C(O)CH_2CH_2), 2.52 (t, 2H, *J* = 7.4, C(O)CH_2CH_2), 2.02 (q, 2H, *J* = 7.1, C(6)H_2), 1.34 (m, 2H, C(7)H_2), 1.24 (m, 20H, CH_2), 0.87 (t, 3H, *J* = 7.1, CH_3); ESI-MS (CH_3OH, relative intensity, %) *m*/*z* 887.0 ($[2M+Na]^+$, 100), 864.8($[2M+H]^+$, 35), 433.0 (MH^+, 4). Calcd for $C_{26}H_{44}N_2O_3$ *m*/*z* 432.3. Anal. Calcd for $C_{26}H_{44}N_2O_3$ (432.64): C, 72.18; H, 10.25; N, 6.48. Found: C, 71.44; H, 10.29; N, 6.45.

4.1.2. General procedure C for the preparation of CCPS analogs. Mixtures of **6**–**18** (0.50 mmol), anhydrous pyridine (2 mL), and anhydrous toluene (2 mL) were heated in a sealed glass test-tube in an oil bath at 75–85 °C over 4.5 h. After completion, the reaction mixture was cooled and evaporated to dryness. The afforded residues were dried under the high vacuum (~1 torr at rt over 6 h) and crystallized to give pure products.

4.1.2.1. D-*erythro*-2-*N*-[2′-(1″-Pyridinium)-acetyl]-sphingosine Bromide (LCL150). Prepared from **6**. Crude product was crystallized from anhydrous ethanol–acetone (1:5, v/v) to give a pure **LCL150** in 72% yield as a pale-brown microcrystalline powder, mp >104 °C (decomp.); TLC ($CHCl_3$/$(CH_3)_2$ CO–MeOH–CH_3COOH–H_2O, 20:8:6:2:1, v/v) R_f 0.15; RP TLC (C18 Silica, CH_3CN–MeOH–1 M NH_4Cl (aq), 4:1:1.5, v/v) R_f 0.44; $[\alpha]_D^{22}$ −7.8° (*c* 1, $CHCl_3$) and −15.7° (*c* 1, MeOH); $[\alpha]_{365}^{22}$ −30.0° (*c* 1, $CHCl_3$) and −61.3° (*c* 1, MeOH); ^{1}H NMR (500 MHz, CD_3OD) δ 8.89 (dd, 2H, *J* = 6.8, 1.3, 2,6-H_{Py}) 8.66 (dt, 1H, *J* = 7.8, 1.3, 4-H_{Py}), 8.14 (t, 2H, *J* = 6.8, 3,5-H_{Py}), 5.73 (dtd, 1H, *J* = 15.3, 6.7, 0.9, 5-H), 5.45 (ddt, 1H, *J* = 15.3, 6.5, 1.0, 4-H), 5.43(d, 2H, *J* = 6.9, CH_2-pyridinium ring), 4.16 (t, 1H, *J* = 6.7, 3-H), 3.98 (m, 1H, 2-H), 3.73 (dd, 1H, *J* = 11.3, 4.3, 1-Ha), 3.63 (dd, 1H, *J* = 11.3, 7.3, 1Hb), 2.05 (q, 2H, *J* = 6.9, C(6)H_2), 1.39 (m, 2H, C(7)H_2), 1.28 (m, 20H, CH_2), 0.89 (t, 3H, J = 7.1, CH_3); (D_2O) δ 8.92 (d, 2H, *J* = 6.0, 2,6-H_{Py}), 8.72 (t, 1H, *J* = 7.8, 4-H_{Py}), 8.20 (t, 2H, *J* = 6.7, 3,5-H_{Py}), 5.86 (m, 1H, 5-H), 5.60 (m, 1H, 4-H), 4.67 (m, 2H, CH_2-pyridinium ring), 4.35 (m, 1H, 3-H), 4.12 (m, 1H, 2-H), 3.82 (dd, 1H, *J* = 8.5, 2.3, 1-Ha), 3.63 (dd, 1H, *J* = 8.5, 5.1, 1Hb), 2.11 (q, 2H, *J* = 7.0, C(6)H_2), 1.43 (m, 2H, C(7)H_2), 1.34 (m, 20H, CH_2), 0.93 (t, 3H, *J* = 7.0, CH_3); ^{13}C NMR (CD_3OD) δ 166.0 (C=O), 147.6 (C4$_{Py}$), 147.4 (C2,6$_{Py}$), 135.1 (*C4*=C5), 130.2 (C4=*C5*), 128.9 (C3,5$_{Py}$), 128.7 (*C*H_2-pyridinium ring), 73.3 (C3), 61.7 (C1), 57.8 (C2), 33.4 (C4=C5*C6*), 33.0, 30.75, 30.72, 30.6, 30.43 and 30.32 (C7–C16), 23.7 (C17), 14.4 (CH_3); ESI-MS (CH_3OH, relative intensity, %) *m*/*z* 419.4 (M^+, 100). Calcd

for $[C_{25}H_{43}N_2O_3]^+$ *m/z* 419.3; Anal. Calcd for $C_{25}H_{43}BrN_2O_3$ (499.5): C, 60.11; H, 8.68; N, 5.61; Br, 16.0. Found: C, 59.52; H, 8.77; N, 5.49; Br, 15.61.

4.1.2.2. D-*erythro*-2-*N*-[2′-(1″-Pyridinium)-acetyl]-4,5-dihydrosphingosine bromide (LCL319). Prepared from **7**. Crude product was crystallized from anhydrous ethanol–acetone (1:5, v/v) to give a pure **LCL319** in 80% yield as a white microcrystalline powder, mp 119–121 °C; TLC ($CHCl_3$–$(CH_3)_2CO$–MeOH–CH_3COOH–H_2O, 20:8:6:2:1, v/v) R_f 0.15; RP TLC (C18 Silica, CH_3CN–MeOH–1 M NH_4Cl (aq), 4:1:1.5, v/v) R_f 0.34; $[\alpha]_D^{22}$ −6.0° (*c* 0.5, MeOH); $[\alpha]_{365}^{22}$ −28.0° (*c* 0.5, MeOH); ^{1}H NMR (500 MHz, $CDCl_3$) δ 9.32 (d, 2H, J = 5.6, 2,6-H_{Py}), 8.70 (br s, 1H, NH), 8.44 (t, 1H, J = 6.0, 4-H_{Py}), 8.02 (t, 2H, J = 6.8, 3,5-H_{Py}), 6.02 (m, 2H, CH_2-pyridinium ring), 4.00 (dd, 1H, J = 11.1, 3.5, 1-Ha), 3.85 (m, 1H, 2-H), 3.80 (m, 2H, 3-H and 1-Hb), 1.59 (m, 2H, C(4)H_2), 1.49 (m, 2H, C(5)H_2), 1.25 (m, 24H, CH_2), 0.88 (t, 3H, J = 7.0, CH_3); (D_2O) δ 8.75 (d, 2H, J = 6.0, 2,6-H_{Py}) 8.52 (t, 1H, J = 7.8, 4-H_{Py}), 8.00 (t, 2H, J = 7.1, 3,5-H_{Py}), 5.48 (br s, 2H, CH_2-pyridinium ring), 3.93 (m, 1H, 3-H), 3.65 (m, 3H, 1Hab and 2-H), 1.40 (m, 2H, C(4)H_2), 1.34 (m, 26H, CH_2), 0.74 (t, 3H, J = 7.0, CH_3); ESI-MS (CH_3OH, relative intensity, %) *m/z* 421.4 (M^+, 100). Calcd for $[C_{25}H_{45}N_2O_3]^+$ *m/z* 421.3; Anal. Calcd for $C_{25}H_{43}BrN_2O_3$ (501.5): C, 59.87; H, 9.04; N, 5.59; Br, 15.93. Found: C, 59.71; H, 9.09; N, 5.55; Br, 15.93.

4.1.2.3. D-*erythro*-2-*N*-[6′-(1″-Pyridinium)-hexanoyl]-sphingosine bromide (LCL29). Prepared from **8**. Crude product was washed with *n*-hexane–ethyl acetate (2× 5 mL, 1:4, v/v/) and anhydrous ethyl acetate (2× 5 mL) following crystallization from anhydrous ethyl acetate–acetone (1:2, v/v) to give a pure **LCL29** in 82% yield as a white slightly hygroscopic microcrystalline powder. TLC ($CHCl_3$–$(CH_3)_2CO$–MeOH–CH_3COOH–H_2O, 20:8:6:2:1, v/v) R_f 0.19; RP TLC (C18 Silica, CH_3CN–MeOH–1 M NH_4Cl (aq), 4:1:1.5 v/v) R_f 0.39; $[\alpha]_D^{22}$ −3.20° (*c* 1, $CHCl_3$) and −14.0° (*c* 1, MeOH); $[\alpha]_{365}^{22}$ −15.0° (*c* 1, $CHCl_3$) and −50.0° (*c* 1, MeOH); ^{1}H NMR (500 MHz, $CDCl_3$) δ 9.40 (d, 2H, J = 5.8, 2,6-H_{Py}) 8.46 (t, 1H,J = 7.6 4-H_{Py}), 8.08 (t, 2H, J = 7.1, 3,5-H_{Py}), 7.72 (d, 1H, J = 7.0, NH), 5.72 (dtd, 1H, J = 15.4, 6.7, 0.6, 5-H), 5.49 (ddt, 1H, J = 15.4, 6.7, 1.1, 4-H), 4.8 (m, 2H, C(6)H_2-pyridinium ring), 4.30 (m, 1H, 3-H), 3.85 (m, 2H, 2-H and 1-Ha), 3.69 (d, 1H, J = 11.3, 1-Hb), 2.34 (m, 2H, COCH_2), 2.15 (m, 2H, C(5)H_2C(6)H_2-pyridinium ring), 2.0 (q, 2H, J = 7.2, C(6)H_2), 1.77 (m, 2H, $COCH_2CH_2$), 1.49 (m, 2H, C(4)H_2C(5)H_2C(6)H_2-pyridinium ring), 1.33 (m, 2H, C(7)H_2), 1.27 (m, 20H, CH_2), 0.87 (t, 3H, J = 6.9, CH_3); (CD_3OD) δ 9.01 (d, 2H, J = 6.4, 2,5-H_{Py}) 8.59 (t, 1H, J = 7.7, 4-H_{Py}), 8.11 (t, 2H, J = 6.8, 3,5-H_{Py}), 7.71 (d, 1H, J = 8.8, NH), 5.68 (dtd, 1H, J = 15.4, 6.8, 0.7, 5-H), 5.45 (ddt, 1H, J = 15.4, 7.3, 1.2, 4-H), 4.63 (t, 2H, J = 7.6, C(6)H_2-pyridinium ring), 4.06 (t, 1H, J = 6.9, 3-H), 3.88 (m, 1H, 2-H), 3.67 (dd, 1H, J = 11.4, 4.2, 1-Ha), 3.64 (dd, 1H, J = 11.4, 6.5, 1-Hb), 2.24 (m, 2H, COCH_2), 2.02 (m, 4H, C(5)(H_2)C(6)H_2-pyridinium ring and C(6)H_2), 1.67 (m, 2H, $COCH_2CH_2$), 1.40 (m, 4H, C(4)(H_2)C(5)(H_2) C(6)H_2-pyridinium ring and C(7)H_2), 1.27 (m, 20H, CH_2), 0.89 (t, 3H, J = 7.0, CH_3); (D_2O) δ 8.96 (d, 2H, J = 6.4, 2,6-H_{Py}), 8.*60* (dt, 1H, J = 7.8, 1.1, 4-H_{Py}), 8.14 (t, 2H, J = 6.8, 3,5-H_{Py}), 5.65 (dtd, 1H, J = 15.1, 6.8, 0.8, 5-H), 5.45 (ddt, 1H, J = 15.1, 6.8, 1.3, 4-H), 4.69 (t, 2H, J = 7.4, C(6)H_2-pyridinium ring), 4.21 (t, 1H, J = 6.1, 3-H), 3.95 (m, 1H, 2-H), 3.74 (dd, 1H, J = 11.5, 2.1, 1-Ha), 3.71 (dd, 1H, J = 11.5, 3.8, 1-Hb), 2.30 (m, 2H, COCH_2), 2.07 (m, 4H, C(5)H_2C(6)H_2-pyridinium ring and C(6)H_2), 1.68 (m, C(7)H_2), 1.44 (m, 4H, C(4)H_2C(5)H_2C(6)H_2-pyridinium ring and $COCH_2CH_2$), 1.29 (m, 20H, CH_2), 0.89 (t, 3H, J = 7.1, CH_3); ^{13}C-NMR (CD_3OD) δ 175.8 (C═O), 147.0 ($C4_{Py}$), 146.1 ($C2,6_{Py}$), 134.8 (*C4*═C5), 131.2(C4═*C5*), 129.6 ($C3,5_{Py}$), 73.9 (C3), 62.9 (*C6*-pyridinium-ring), 62.2 (C1), 57.0 (C2), 36.6 (C═O*C2*), 33.5 (C4═C5*C6*), 33.2 (C9 or C10), 32.1(*C5*C6-pyridinium ring), 30.95, 30.92, 30.83, 30.63, 30.56 and 30.47 (C7–C16), 26.7 (*C4*C5C6-pyridinium ring), 26.1 (C═OC2*C3*), 23.8 (C17), 14.5 (CH_3); ESI-MS (CH_3OH, relative intensity, %) *m/z* 475.4 (M^+, 100). Calcd for $[C_{29}H_{51}N_2O_3]^+$ *m/z* 475.4; Anal. Calcd for $C_{29}H_{51}BrN_2O_3 \cdot H_2O$ (573.65): C, 60.72; H, 9.31; N, 4.88; Br, 13.93. Found: C, 60.19; H, 9.22; N, 4.78; Br, 14.21.

4.1.2.4. L-*threo*-2-*N*-[6′-(1″-Pyridinium)-hexanoyl]-sphingosine bromide (LCL124). Prepared from **9** as **LCL29** in 73% yield. Analytical sample of **LCL124** was obtained by crystallization from anhydrous ethyl acetate–acetone (1:2, v/v) as a white hygroscopic microcrystalline powder. TLC ($CHCl_3$–$(CH_3)_2CO$–MeOH–CH_3COOH–H_2O, 20:8:6:2:1, v/v) R_f 0.17; RP TLC (C18 Silica, CH_3CN–MeOH–1 M NH_4Cl (aq), 4:1:1.5, v/v) R_f 0.38; $[\alpha]_D^{21}$ −6.40° (*c* 1, $CHCl_3$); $[\alpha]_{365}^{21}$ −25.1° (*c* 1, $CHCl_3$); ^{1}H NMR (500 MHz, $CDCl_3$) δ 9.39 (d, 2H, J = 5.6, 2,6-H_{Py}) 8.47 (t, 1H, J = 7.8, 4-H_{Py}), 8.09 (t, 2H, J = 7.5, 3,5-H_{Py}), 7.53 (d, 1H, J = 7.9, NH), 5.72 (dtd, 1H, J = 15.4, 6.7, 0.5, 5-H), 5.49 (ddt, 1H, J = 15.4, 6.7, 1.1, 4-H), 4.88 (t, 2H, J = 7.6, C(6)H_2-pyridinium ring), 4.25 (t, 1H, J = 5.8, 3-H), 3.83 (m, 1H, 2-H), 3.72 (dd, 1H, J = 11.5, 4.0, 1-Ha), 3.67 (dd, 1H, J = 11.5, 5.5, 1-Hb), 2.36 (t, 2H, J = 7.1, COCH_2), 2.14 (m, 2H, C(5)H_2C(6)H_2-pyridinium ring), 1.98 (q, 2H, J = 7.0,C(6)H_2), 1.74 (m, 2H, $COCH_2CH_2$), 1.47 (m, 2H, C(4)H_2C(5)H_2C(6)H_2-pyridinium ring), 1.32 (m, 2H, C(7)H_2), 1.23 (m, 20H, CH_2), 0.86 (t, 3H, J = 6.9, CH_3); (CD_3OD) δ 9.00 (dd, 2H, J = 6.2, 1.2, 2,6-H_{Py}) 8.59 (dt, 1H, J = 7.8, 1.3, 4-H_{Py}), 8.11 (t, 2H, J = 6.8, 3,5-H_{Py}), 7.53 (d, 1H, J = 7.9, NH), 5.70 (dtd, 1H, J = 15.4, 7.0, 1.1, 5-H), 5.43 (ddt, 1H, J = 15.4, 6.7, 1.1, 4-H), 4.63 (t, 2H, J = 7.5, C(6)H_2-pyridinium ring), 4.21 (t, 1H, J = 6.2, 3-H), 3.86 (m, 1H, 2-H), 3.65 (dd, 1H, J = 11.0, 5.8, 1-Ha), 3.50 (dd, 1H, J = 11.0, 6.3, 1-Hb), 2.26 (t, 2H, J = 7.3, COCH_2), 2.02 (m, 4H, C(6)H_2 and C(5)H_2C(6)H_2-pyridinium ring), 1.68 (m, 2H, $COCH_2CH_2$), 1.41 (m, 4H, C(4)H_2C(5)H_2C(6)H_2-pyridinium ring and C(7)H_2), 1.27 (m, 20H, CH_2), 0.89 (t, 3H, J = 6.9, CH_3); (D_2O) δ 8.98 (d, 2H, J = 5.9, 2,6-H_{Py}), 8.*66* (t, 1H, J = 7.6, 4-H_{Py}), 8.19 (t, 2H, J = 6.6, 3,5-H_{Py}), 5.84 (dtd, 1H, J = 15.1, 6.8, 0.8, 5-H), 5.55 (ddt, 1H, J = 15.1, 6.8, 1.3, 4-H), 4.73 (m, 2H, J = 7.5, C(6)H_2-pyridinium ring),

4.31 (t, 1H, J = 5.5, 3-H), 3.97 (m, 1H, 2-H), 3.74 (dd, 1H, J = 11.5, 4.4, 1-Ha), 3.62 (dd, 1H, J = 11.5, 6.6, 1-Hb), 2.38 (m, 2H, COCH_2), 2.12 (m, 4H, C(5)H_2C(6)H_2-pyridinium ring and C(6)H_2), 1.75 (m, C(7)H_2), 1.46 (m, 4H, C(4)H_2C(5)H_2C(6)H_2-pyridinium ring and $COCH_2CH_2$), 1.34 (m, 20H, CH_2), 0.94 (t, 3H, J = 6.4, CH_3); ^{13}C-NMR ($CDCl_3$) δ 174.9 (C═O), 145.5 ($C4_{Py}$), 145.3 ($C2,6_{Py}$), 133.6 (C4═C5), 129.6 (*C4*═C5), 128.8 ($C3,5_{Py}$), 72.8 (C3), 62.9 (C1), 62.0 (*C6*-pyridinium-ring), 56.5 (C2), 35.8(C═O*C2*), 32.66 (C6), 32.16 (C9 or C10), 31.13 (*C5*C6-pyridinium ring), 29.96, 29.92, 29.90, 29.81, 29.62, 29.60 and 29.55 (C8–C17), 25.11 (*C4*C5C6-pyridinium ring), 24.76 (C═OC2*C3*), 22.92 (C7), 14.35 (CH_3); (CD_3OD) δ76.0 (C═O), 146.9 ($C4_{Py}$), 146.1 ($C2,6_{Py}$), 133.9 (*C4*═C5), 131.3 (C4═*C5*), 129.6 ($C3,5_{Py}$), 72.0 (C3), 62.9 (C1), 62.6 (*C6*-pyridinium-ring), 57.0 (C2), 36.6(C═O*C2*), 33.5 (C4═C5*C6*), 33.2 (C9 or C10), 32.1(*C5*C6-pyridinium ring), 30.9, 30.7, 30.6, 30.5, and 30.4 (C8-C17), 26.6 (*C4*C5C6-pyridinium ring), 26.0 (C═OC2*C3*), 23.8 (C4═C5C6*C7*), 14.54 (CH_3); ESI-MS (CH_3OH, relative intensity, %) *m*/*z* 475.4 (M^+, 100). Calcd for $[C_{39}H_{51}N_2O_3]^+$ *m*/*z* 475.4. Anal. Calcd for $C_{29}H_{51}BrN_2O_3 \cdot H_2O$ (573.65): C, 60.72; H, 9.31; N, 4.88; Br, 13.93. Found: C, 60.45; H, 9.09; N, 4.68; Br, 14.01.

4.1.2.5. L-*erythro*-2-*N*-[6′-(1″-Pyridinium)-hexanoyl]-sphingosine bromide (LCL187). Prepared from **10** as **LCL29** in 71% yield. Analytical sample was obtained by crystallization from ethyl acetate–acetone (2:1, v/v/) as a white hygroscopic powder; $[\alpha]_D^{22}$ +3.10° (*c* 1, $CHCl_3$) and +14.5° (*c* 1, MeOH); $[\alpha]_{365}^{22}$ +14.2° (*c* 1, $CHCl_3$) and +51.2° (*c* 1, MeOH). Remaining data are identical as reported for **LCL29**. Anal. Calcd for $C_{29}H_{51}BrN_2O_3 \cdots H_2O$ (573.65): C, 60.72; H, 9.31; N, 4.88; Br, 13.93. Found: C, 60.11; H, 9.12; N, 4.98; Br, 13.71.

4.1.2.6. D-*threo*-2-*N*-[6′-(1″-Pyridinium)-hexanoyl]-sphingosine bromide (LCL272). Prepared from **11** as **LCL124** in 68% yield. Analytical sample was obtained by crystallization from ethyl acetate–acetone (2:1, v/v/) as a white hygroscopic powder; $[\alpha]_D^{22}$ +6.2° (*c* 1, $CHCl_3$); $[\alpha]_{365}^{22}$ +26.0° (*c* 1, $CHCl_3$); remaining data are identical as reported for **LCL124.** Anal. Calcd for $C_{29}H_{51}BrN_2O_3 \cdot H_2O$ (573.65): C, 60.72; H, 9.31; N, 4.88; Br, 13.93. Found: C, 60.23; H, 9.03; N, 4.64; Br, 13.63.

4.1.2.7. D-*erythro*-2-*N*-[6′-(1″-Pyridinium)-hexanoyl]-4,5-dihydrosphingosine bromide (LCL143). Prepared from **12** as **LCL319** in 71% yield. Analytical sample was prepared by crystallization from anhydrous ethyl acetate–acetone (1:1, v/v) as a white microcrystalline powder, mp ~95 °C getting wet and melts with decomposition above 155 °C; TLC ($CHCl_3$–$(CH_3)_2CO$–MeOH–CH_3COOH–H_2O, 20: 8:6:2:1, v/v) R_f 0.20; RP TLC (C18 Silica, CH_3CN–MeOH–1 M NH_4Cl (aq), 4:1:1.5 v/v) R_f 0.30; $[\alpha]_D^{22}$ −0.55° (*c* 0.5, MeOH); $[\alpha]_{365}^{22}$ −3.5° (*c* 0.5, MeOH); ^{1}H NMR (500 MHz, CD_3OD) δ 9.01 (dd, 2H, J = 6.7, 1.2, 2,5-H_{Py}) 8.59 (t, 1H, J = 7.7, 4-H_{Py}), 8.12 (t, 2H, J = 6.8, 3,5-H_{Py}), 4.63 (t, 2H, J = 7.5, C(6)H_2-pyridinium ring), 4.06 (t, 1H, J = 6.9, 3-H), 3.83 (m, 1H, 2-H), 3.70 (dd, 1H, J = 11.2, 4.1, 1-Ha), 3.65 (dd, 1H, J = 11.2, 6.5, 1-Hb), 2.26 (t, 2H, J = 7.2, COCH_2), 2.03 (m, 2H, C(5)H_2C(6)H_2-pyridinium ring), 1.69 (m, 2H, $COCH_2CH_2$), 1.50 (m, 2H, $COCH_2CH_2CH_2$), 1.42 (m, 2H, C(4)H_2), 1.27 (m, 24H, CH_2), 0.89 (t, 3H, J = 7.1, CH_3); (D_2O) 8.99 (d, 2H, J = 5.7, 2,6-H_{Py}), 8.*67* (t, 1H, J = 7.8, 4-H_{Py}), 8.20 (t, 2H, J = 6.8, 3,5-H_{Py}), 4.74 (t, 2H, J = 7.4, C(6)H_2-pyridinium ring), 3.97 (m, 1H, 2-H), 3.80 (m, 3H, 2-H and 1-Hab), 2.40 (m, 2H, COCH_2), 2.07 (m, 2H, C(5)H_2C(6) H_2-pyridinium ring), 1.68 (m, 2H, $COCH_2CH_2$), 1.53 (m, 4H, C(4)H_2C(5)H_2C(6)H_2-pyridinium ring and C(4)H_2), 1.29 (m, 24H, CH_2), 0.93 (t, 3H, J = 6.5, CH_3); ESI-MS (CH_3OH, relative intensity, %) *m*/*z* 477.3 (M^+, 100). Calcd for $[C_{29}H_{53}N_2O_3]^+$ *m*/*z* 477.4. Anal. Calcd for $C_{29}H_{53}BrN_2O_3$ (557.65): C, 62.46; H, 9.58; N, 5.02; Br, 14.33. Found: C, 59.98; H, 9.60; N, 4.80; Br, 14.19.

4.1.2.8. D-*erythro*-2-*N*-[12′-(1″-Pyridinium)-dodecanoyl]-sphingosine bromide (LCL88). Prepared from **13** as **LCL150** in 74% yield. Analytical sample was prepared by crystallization from anhydrous ethyl acetate–acetone (2:1, v/v) as a white microcrystalline powder, mp 79–80 °C; TLC ($CHCl_3$–$(CH_3)_2CO$–MeOH/CH_3COOH–H_2O, 20:8:4:2:1, v/v) R_f 0.28; RP TLC (C18 Silica, CH_3CN–MeOH–1 M NH_4Cl (aq), 4:1:1.5 v/v) R_f 0.38; $[\alpha]_D^{20}$ −0.51° (*c* 1, $CHCl_3$) and −12.9° (*c* 1, MeOH); $[\alpha]_{365}^{20}$ −8.50° (*c* 1, $CHCl_3$) and −48.5° (*c* 1, MeOH); ^{1}H NMR (500 MHz, $CDCl_3$) δ 9.40 (d, 2H, J = 6.0, 2,6-H_{Py}) 8.48 (t, 1H,J = 7.4, 4-H_{Py}), 8.12 (t, 2H, J = 6.9, 3,5-H_{Py}), 7.14 (d, 1H, J = 7.0, NH), 5.74 (dtd, 1H, J = 15.3, 6.7, 0.6, 5-H), 5.52 (ddt, 1H, J = 15.3, 6.7, 1.1, 4-H), 4.94 (t, 2H, J = 7.5, C(12)H_2-pyridinium ring), 4.29 (m, 1H, 3-H), 3.89 (m, 2H, 2-H and 1-Ha), 3.68 (dd, 1H, J = 13.0, 4.5, 1-Hb), 2.28 (t, 2H, J = 7.4, COCH_2), 2.05 (m, 4H, C(11)H_2C(12)H_2-pyridinium ring and C(6)H_2), 1.63 (m, 2H, $COCH_2CH_2$), 1.24 (m, 36H, CH_2), 0.86 (t, 3H, J = 7.3, CH_3); (CD_3OD) δ 9.01 (dd, 2H, J = 6.7, 1.3, 2,5-H_{Py}) 8.61 (tt, 1H, J = 7.8, 1.3 4-H_{Py}), 8.11 (t, 2H, J = 7.8, 3,5-H_{Py}), 7.60 (d, ~0.2H, J = 8.2, NH), 5.68 (dtd, 1H, J = 15.2, 6.6, 0.7, 5-H), 5.45 (ddt, 1H, J = 15.2, 7.4, 1.2, 4-H), 4.62 (t, 2H, J = 7.6, C(12)H_2-pyridinium ring), 4.04 (t, 1H, J = 7.3, 3-H), 3.85 (m, 1H, 2-H), 3.68 (d, 2H, J = 5.1, 1-Ha,b), 2.18 (t, 2H, J = 7.1, COCH_2), 2.01 (m, 4H, C(11)H_2 C(12)H_2-pyridinium ring and C(6)H_2), 1.57 (m, 2H, $COCH_2CH_2$), 1.38 (m, 4H, C(10)H_2C(11)H_2C(12) H_2-pyridinium ring and C(7)H_2), 1.27 (m, 32H, CH_2), 0.88 (t, 3H, J = 7.1, CH_3); (D_2O) δ 9.03 (d, 2H, J = 6.1, 2,6-H_{Py}), 8.*72* (t, 1H, J = 7.9, 4-H_{Py}), 8.24 (t, 2H, J = 5.5, 3,5-H_{Py}), 5.80 (dtd, 1H, J = 15.0, 6.8, 0.8, 5-H), 5.55 (ddt, 1H, J = 15.0, 6.8, 1.3, 4-H), 4.78 (t, 2H,J = 7.3, C(12)H_2-pyridinium ring), 4.20 (t, 1H, J = 7.0, 3-H), 3.96 (m, 1H, 2-H), 3.87 (bs, 2H, 1-Ha,b), 2.29 (t, J = 5.5, 2H, COCH_2), 2.09 (m, 4H, C(11)H_2C(12)H_2-pyridinium ring and C(6)H_2), 1.62 (m, C(7)H_2), 1.43 (m, 4H, C(10)H_2C(11)H_2C(12)H_2-pyridinium ring and $COCH_2CH_2$), 1.32 (m, 32H, CH_2), 0.92 (t, 3H, J = 6.7, CH_3); ^{13}C NMR (CD_3OD) δ 176.43 (C═O), 147.04 ($C4_{Py}$), 146.1 ($C2,6_{Py}$), 134.86 (*C4*═C5), 131.42(C4═*C5*), 129.67 ($C3,5_{Py}$), 73.8 (C3), 63.27 (*C12*-pyridinium-ring), 62.44(C1), 56.9 (C2), 37.45 (C═O*C2*), 33.58 (C4═C5*C6*), 33.24 (C15 or

C16?), 32.66(*C11*C12-pyridinium ring), 30.97, 30.94, 30.92, 30.86, 30.72, 30.68, 30.63, 30.54, 30.52 and 30.25 (C6–C16), 27.34 (*C*10C11C12-pyridinium ring), 27.2 (C═OC2*C3*), 23.9 (C17), 14.61(CH_3) ; ESI-MS (CH_3OH, relative intensity, %) *m/z* 559.4 (M^+, 100). Calcd for $[C_{35}H_{63}N_2O_3]^+$ *m/z* 559.5. Anal. Calcd for $C_{35}H_{63}BrN_2O_3$ (639.8): C, 65.71; H, 9.93; N, 4.38; Br, 12.49. Found: C, 65.32; H, 9.94; N, 4.30; Br, 12.10.

4.1.2.9. D-*erythro*-2-*N*-[12′-(1″-Pyridinium)-dodecanoyl]-4,5-dihydrosphingosine bromide (LCL249). Prepared from **14** as **LCL319** in 72% yield. Analytical sample was prepared by crystallization from anhydrous ethyl acetate–acetone (2:1, v/v) as a white microcrystalline powder, mp 69–71 °C; TLC ($CHCl_3$–$(CH_3)_2CO$–MeOH–CH_3COOH–H_2O, 20:8:4:2:1, v/v) R_f 0.29; RP TLC (C18 Silica, CH_3CN–MeOH–1 M NH_4Cl (aq), 4:1:1.5 v/v) R_f 0.26; $[\alpha]_D^{21}$ +7.0° (*c* 1, $CHCl_3$); $[\alpha]_{365}^{22}$ +17.4° (*c* 1, $CHCl_3$); ^1H NMR (500 MHz, $CDCl_3$) δ 9.41 (d, 2H, $J = 5.6$, 2,6-H_{Py}), 8.49 (t, 1H, $J = 7.7$, 4-H_{Py}), 8.13 (t, 2H, $J = 7.5$, 3,5-H_{Py}), 7.31 (d, 1H, $J = 7.8$, NH), 4.93 (t, 2H, $J = 7.5$, C(12)H_2-pyridinium ring), 3.93 (dd, 1H, $J = 11.5$, 4.5, 1-Ha), 3.82 (m, 1H, 2-H), 3.74 (m, 1H, 3-H), 3.70 (dd, 1H, $J = 11.5$, 3.0, 1-Hb), 2.28 (t, 2H, $J = 7.5$, $COCH_2$), 2.05 (m, 2H, C(11)H_2C(12)H_2-pyridinium ring), 1.63 (m, 2H, $COCH_2CH_2$), 1.49 (m, 2H, C(4)H_2), 1.23 (m, 40H, CH_2), 0.86 (t, 3H, $J = 7.1$, CH_3); (CD_3OD) δ 9.01 (dd, 2H, $J = 6.6$, 1.2, 2,6-H_{Py}), 8.59 (dt, 1H, $J = 6.8$, 1,2, 4-H_{Py}), 8.11 (t, 2H, $J = 6.9$, 3,5-H_{Py}), 4.62 (t, 2H, $J = 7.6$, C(12)H_2-pyridinium ring), 3.81 (m, 1H, 2-H), 3.70 (dd, 1H, $J = 11.2$, 4.3, 1-Ha), 3.68 (dd, 1H, $J = 11.4$, 6.0, 1-Hb), 3.58 (m, 1H, 3-H), 2.21 (t, 2H, $J = 7.5$, $COCH_2$), 2.01 (m, 2H, C(11)H_2C(12)H_2-pyridinium ring), 1.60 (m, 2H, $COCH_2CH_2$), 1.52 (m, 2), 1.38 (m, 4H, C(10)H_2C(11)H_2C(12)H_2-pyridinium ring C(4)H_2), 1.27 (m, 36H, CH_2), 0.89 (t, 3H, $J = 7.1$, CH_3); ^{13}C-NMR (CD_3OD) δ 176.43 (C═O), 146.9 ($C4_{Py}$), 146.04 (C2,6_{Py}), 129.6 (C3,5_{Py}), 72.4 (C3), 63.2 (*C12*-pyridinium-ring), 62.5 (C1), 56.8 (C2), 37.3 (CO*C2*), 35.0 (C4) 33.18 (C15?), 32.61 (*C*11C12-pyridinium ring), 30.9, 30.83, 30.65, 30.6, 30.57, 30.51, 30.42, 30,36 and 30.2 (C8–C15 and C4–C9), 26.6 (*C*10C11C12-pyridinium ring), 27.16 (COC2*C3*), 26.77 (C16), 23.8 (C17), 14.54 (CH_3); ESI-MS (CH_3OH, relative intensity, %) *m/z* 561.4 (M^+, 100). Calcd for $[C_{35}H_{65}N_2O_3]^+$ *m/z* 561.5. Anal. Calcd for $C_{35}H_{63}BrN_2O_3$ (639.8): C, 65.50; H, 10.21; N, 4.36; Br, 12.45. Found: C, 65.19; H, 10.14; N, 4.32; Br, 12.35.

4.1.2.10. D-*erythro*-2-*N*-[16′-(1″-Pyridinium)-hexadecanoyl]-sphingosine bromide (LCL30). Prepared from **15** (2.15 g, 3.48 mmol), anhydrous pyridine (10 mL) and anhydrous toluene (8 mL) according to the Procedure C. The obtained mixture was cooled to room temperature, diluted with ethyl acetate (20 mL), and left in the refrigerator (+4 °C) for 6 h. The formed precipitate was separated by filtration, washed with ethyl acetate–acetone (10 mL, 1:1, v/v), and dried to give crude product (2.31 g). This material was crystallized from acetone–ethanol (5:1, v/v) to give **LCL30** (2.16 g, 89%) as a white microcrystalline powder, mp 116–118 °C; TLC ($CHCl_3$–$(CH_3)_2CO$–MeOH–CH_3COOH–H_2O, 20:8:4:2:1, v/v) R_f 0.33; RP TLC (C18 Silica, CH_3CN–MeOH–1 M NH_4Cl (aq), 4:1:1.5, v/v); R_f 0.22; $[\alpha]_D^{22}$ −1.20° (*c* 1, $CHCl_3$) and −9.0° (*c* 1, MeOH); $[\alpha]_{365}^{22}$ −11.8° (*c* 1, $CHCl_3$) and −36.0° (*c* 1, MeOH); $[\alpha]_D^{37}$ −12.0° (*c* 1, EtOH/H_2O, 9:1, v/v/); $[\alpha]_{365}^{37}$ −56.0° (*c* 1, EtOH–H_2O, 9:1,v/v); ^1H NMR (500 MHz, $CDCl_3$) δ 9.37 (d, 2H, $J = 6.0$, 2,6-H_{Py}) 8.47 (t, 1H, $J = 7.8$, 4-H_{Py}), 8.11 (t, 2H, $J = 7.1$, 3,5-H_{Py}), 6.80 (d, 1H, $J = 6.7$, NH), 5.73 (dtd, 1H, $J = 15.2$, 6.6, 0.6, 5-H), 5.52 (ddt, 1H, $J = 15.2$, 6.5, 1.2, 4-H), 4.96 (t, 2H, $J = 7.5$, C(16)H_2-pyridinium ring), 4.30 (m, 1H, 3-H), 3.93 (dd, 2H, $J = 11.1$, 4.5, 1-Ha), 3.91 (m, 2H, 2-H), 3.69 (dd, 1H, $J = 11.1$, 2.7, 1-Hb), 2.29 (t, 2H, $J = 7.4$, $COCH_2$), 2.06 (m, 4H, C(15)H_2C(16)H_2-pyridinium ring and C(6)H_2), 1.65 (m, 2H, $COCH_2CH_2$), 1.26 (m, 44H, CH_2), 0.88 (t, 3H, $J = 7.1$, CH_3); (CD_3OD) δ 9.00 (dd, 2H, $J = 5.5$, 1.2, 2,5-H_{Py}) 8.59 (tt, 1H, $J = 7.8$, 1.2 4-H_{Py}), 8.11 (t, 2H, $J = 7.0$, 3,5-H_{Py}), 5.68 (dtd, 1H, $J = 15.3$, 6.7, 0.8, 5-H), 5.44 (ddt, 1H, $J = 15.3$, 7.5, 1.3, 4-H), 4.63 (t, 2H, $J = 7.5$, C(16)H_2-pyridinium ring), 4.04 (t, 1H, $J = 7.4$, 3-H), 3.84 (dt, 1H, $J = 7.5$, 5.0, 2-H), 3.67(d, 2H, $J = 5.1$, 1-Ha,b), 2.18 (t, 2H, $J = 7.5$, $COCH_2$), 2.03 (m, 4H, C(15)H_2C(16)H_2-pyridinium ring and C(6)H_2), 1.57 (m, 2H, $COCH_2CH_2$), 1.38 (m, 4H, C(14)H_2C(15)H_2C(16)H_2-pyridinium ring and C(7)H_2), 1.27 (m, 40H, CH_2), 0.88 (t, 3H, $J = 7.0$, CH_3); (D_2O) δ 9.01 (d, 2H, $J = 6.4$, 2,6-H_{Py}), 8.*68* (t, 1H, $J = 7.6$, 4-H_{Py}), 8.20 (t, 2H, $J = 5.8$, 3,5-H_{Py}), 5.75 (dtd, 1H, $J = 15.1$, 6.6, 0.8, 5-H), 5.48 (ddt, 1H, $J = 15.1$, 6.8, 1.2, 4-H), 4.73 (t, 2H, J = 7.3, C(16)H_2-pyridinium ring), 4.11 (t, 1H, $J = 6.9$, 3-H), 3.87 (m, 1H, 2-H), 3.78 (br s, 2H, 1-Ha,b), 2.25 (t, 2H, $J = 5.5$, 2H, $COCH_2$), 2.06 (m, 4H, C(15)H_2C(16)H_2-pyridinium ring and C(6)H_2), 1.58 (m, C(7)H_2), 1.39 (m, 4H, C(14)H_2C(15)H_2C(16)H_2- pyridinium ring and $COCH_2CH_2$), 1.29 (m, 32H, CH_2), 0.85 (t, 3H, $J = 6.7$, CH_3); ESI-MS (CH_3OH, relative intensity, %) *m/z* 615.6 (M^+, 100). Calcd for $[C_{39}H_{71}N_2O_3]^+$ *m/z* 615.5. Anal. Calcd for $C_{39}H_{71}BrN_2O_3$ (695.9): C, 67.3; H, 10.28; N, 4.03; Br, 11.48. Found: C, 67.03; H, 10.34; N, 4.06; Br, 11.26.

4.1.2.11. L-*erythro*-2-*N*-[16′-(1″-Pyridinium)-hexadecanoyl]-sphingosine bromide (LCL255). Prepared from **18** as **LCL30** in 82% yield. Analytical sample was obtained by crystallization from acetone–ethanol (5:1, v/v/) as a white hygroscopic powder; $[\alpha]_D^{20}$ +12.0° (*c* 1, MeOH); $[\alpha]_{365}^{20}$ +44.2° (*c* 1, MeOH). Remaining data are identical as reported for **LCL30**. Anal. Calcd for $C_{39}H_{71}BrN_2O_3$ (695.9): C, 67.3; H, 10.28; N, 4.03; Br, 11.48. Found: C, 67.22; H, 10.05; N, 4.11; Br, 11.31.

4.1.2.12. L-*threo*-2-*N*-[16′-(1″-Pyridinium)-hexadecanoyl]-sphingosine bromide (LCL87). Prepared from **17** as **LCL30** in 80% yield. Analytical sample of **LCL87** was prepared by crystallization from acetone–ethanol (5:1, v/v) as a white microcrystalline powder, mp 113–115 °C; TLC ($CHCl_3$–$(CH_3)_2CO$–MeOH–CH_3COOH–H_2O, 20:8:4:2:1, v/v); R_f 0.32; RP TLC (C18 Silica, CH_3CN–MeOH–1 M NH_4Cl (aq), 4:1:1.5, v/v) R_f 0.23; $[\alpha]_D^{22}$ −12.1° (*c* 1, MeOH); $[\alpha]_{365}^{22}$ −46.8° (*c* 1, MeOH); ^1H NMR (500 MHz, $CDCl_3$) δ 9.33 (d, 2H, $J = 6.0$, 2,6-

H_{Py}) 8.44 (t, 1H, J = 7.8, 4-H_{Py}), 8.08 (t, 2H, J = 7.0, 3,5-H_{Py}), 6.51 (d, 1H, J = 7.8, NH), 5.69 (dtd, 1H, J = 15.2, 6.6, 0.6, 5-H), 5.42 (ddt, 1H, J = 15.2, 6.5, 1.2, 4-H), 4.92 (t, 2H, J = 7.5, C(16)H_2-pyridinium ring), 4.35 (t, 1H, J = 4.5, 3-H), 3.84 (m, 1H, 2-H), 3.70 (m, 2H, 1-Ha,b), 2.21 (t, 2H, J = 7.4, COCH_2), 2.01 (m, 4H, C(15)H_2C(16)H_2-pyridinium ring and C(6)H_2), 1.58 (m, 2H, $COCH_2CH_2$), 1.22 (m, 44H, CH_2), 0.84 (t, 3H, J = 7.0, CH_3); ESI-MS (CH_3OH, relative intensity, %) m/z 615.6 (M^+, 100). Calcd for $[C_{39}H_{71}N_2O_3]^+$ m/z 615.5. Anal. Calcd for $C_{39}H_{71}BrN_2O_3$(695.9): C, 67.3; H, 10.28; N, 4.03; Br, 11.48. Found: C, 67.03; H, 10.21; N, 4.00; Br, 11.44.

4.1.2.13. D-*erythro*-2-*N*-[16′-(1″-Pyridinium)-hexadecanoyl]-4,5-dihydrosphingosine bromide (LCL345). Prepared from **16** as **LCL30** in 79% yield. Analytical sample of **LCL345** was prepared by crystallization from acetone/ethanol (5:1, v/v) as a white microcrystalline powder, mp 100–101 °C; TLC ($CHCl_3$–$(CH_3)_2CO$–MeOH–CH_3COOH–H_2O, 20:8:4:2:1, v/v) R_f 0.36; RP TLC (C18 Silica, CH_3CN–MeOH–1 M NH_4Cl (aq), 4:1:1.5, v/v) R_f 0.15; $[\alpha]_D^{22}$ +3.4° (c 0.5, MeOH); $[\alpha]_{365}^{22}$ +3.3° (c 0.5, MeOH); ^{1}H NMR (500 MHz, $CDCl_3$) δ 9.27 (d, 2H, J = 5.8 2,6-H_{Py}), 8.41 (t, 1H, J = 7.7, 4-H_{Py}), 8.05 (t, 2H, J = 7.0, 3,5-H_{Py}), 7.18 (m, 1H, NH), 4.88 (t, 2H, J = 7.6, C(16)H_2-pyridinium ring), 3.91 (dd, 1H, J = 11.6, 5.2, 1-Ha), 3.78 (m, 1H, 2-H), 3.71 (m, 1H, 3-H), 3.65 (dd, 1H, J = 11.6, 2.8, 1-Hb), 2.26 (t, 2H, J = 7.7, $COCH_2$), 2.0 (m, 2H, C(15)H_2C(16)H_2-pyridinium ring), 1.60 (m, 2H, $COCH_2CH_2$), 1.44 (m, 2H, C(4)H_2), 1.21 (m, 44H, CH_2), 0.80 (t, 3H, J = 7.0, CH_3); (CD_3OD) δ 9.01 (dd, 2H, J = 6.6, 1.2, 2,6-H_{Py}), 8.61 (dt, 1H, J = 6.8, 1.2, 4-H_{Py}), 8.11 (t, 2H, J = 7.0, 3,5-H_{Py}), 4.62 (t, 2H, J = 7.6, C(16)H_2-pyridinium ring), 3.81 (m, 1H, 2-H), 3.68 (m, 2H, 1-Hab), 3.57 (m, 1H, 3-H), 2.21 (t, 2H, J = 7.5, COCH_2), 2.01 (m, 2H, C(15)H_2C(16)H_2-pyridinium ring), 1.57 (m, 4H, $COCH_2CH_2$ C(14)H_2C(15)H_2C(16)H_2-pyridinium ring), 1.27 (m, 36H, CH_2), 0.89 (t, 3H, J = 7.1, CH_3); (D_2O) δ 9.01 (br s, 2H, 2,6-H_{Py}), 8.73 (t, 1H, J = 7.8, 4-H_{Py}), 8.26 (t, 2H, J = 7.1, 3,5-H_{Py}), 4.80 (t, 2H, J = 7.1, C(16)H_2-pyridinium ring), 3.91 (m, 2H, 1-Hab), 3.82 (m, 1H, 2-H), 3.70 (m, 1H, 3-H), 2.39 (m, 2H, COCH_2), 2.11 (m, 2H, C(15)H_2C(16)H_2-pyridinium ring), 1.65 (m, 4H, $COCH_2CH_2$ C(14)H_2C(15)H_2C(16)H_2-pyridinium ring), 1.32 (m, 36H, CH_2), 0.90 (t, 3H, J = 6.9, CH_3); ^{13}C-NMR (CD_3OD) δ 176.5 (C=O), 147.02 ($C4_{Py}$), 146.09 ($C2,6_{Py}$), 129.7 ($C3,5_{Py}$), 72.43 (C3), 63.27 (*C16*-pyridinium-ring), 62.6 (C1), 56.92 (C2), 37.43(CO*C2*), 35.13 (COC2*C3* and C4), 33.24, 32.7 (*C15*C16-pyridinium ring), 30.84, 30.79, 30.73, 30.67, 30.64, 30.51 and 30.28, (C5–C15 and C5–C13), 27.36 (*C14*C15C16-pyridinium ring), 27.26 (COC2C3*C4*), 26.78(C16), 23.9 (C17), 14.61 (CH_3); ESI-MS (CH_3OH, relative intensity, %) m/z 617.7 (M^+, 100). Calcd for $[C_{39}H_{73}N_2O_3]^+$ m/z 617.6. Anal. Calcd for $C_{39}H_{73}BrN_2O_3$ (697.9): C, 67.12; H, 10.54; N, 4.01; Br, 11.45. Found: C, 66.93; H, 10.45; N, 3.91; Br, 11.19.

4.1.2.14. D-*erythro*-2-*N*-[6′-[1″-[4‴-[(4‴′-*N*,*N*- Dimethylamino)-styryl]-pyridinium]-hexanoyl]]-sphingosine bromide (LCL186). Prepared from **8** (167 mg, 0.35 mmol) and 4-[4′-(*N*,*N*-dimethylamino)-styryl]-pyridine (314 mg, 1.4 mmol) according to the Procedure C with the reaction time extended to 70 h. Reaction mixture was concentrated to the half of the volume and left in the refrigerator overnight. The red precipitate was filtered, washed twice with ethyl acetate, and dried under vacuum. This material was treated with a warm (~45 °C) mixture of ethanol–chloroform (10 mL, 2: 3, v/v), sonicated for 10 min, and filtered off to separate the excess of unreacted 4-[4′-(*N*,*N*-dimethylamino)-styryl]-pyridine. The collected washings and extracts were concentrated to a volume of 3 mL and subjected to a two-step flash chromatography. Elution with $CHCl_3$–EtOH (3:2, v/v) delivered the less polar side-by products and the starting materials. After changing the eluent system to $CHCl_3$–MeOH (3:2, v/v), a pure product was obtained as a red solid (131 mg, 53% yield). Analytical sample of **LCL186** was obtained by crystallization from acetone as a deep orange microcrystalline powder, mp >105 °C (decomp.); TLC ($CHCl_3$–$(CH_3)_2CO$–EtOH–CH_3COOH–H_2O, 20:8:6:2:1, v/v) R_f 0.40; RP TLC (C18 Silica, CH_3CN–MeOH–1 M NH_4Cl (aq), 4:1:1.5, v/v) R_f 0.40; UV–vis (50% EtOH) λ_{max} (logε) 481.5 nm (4.72); fluorescence (E_m, 50% EtOH) λ_{max} (rel. int.) = 525 nm (2.0); ^{1}H NMR (500 MHz, $CDCl_3$) δ 8.84 (d, 2H, J = 7.7, 2-H_{Py}), 7.98 (d, 1H, J = 4.7, NH), 7.77 (d, 2H, J = 7.7, 3-H_{Py}), 7.60 (d, 1H, J = 15.9, Ar-CH=C*H*-pyridinium ring), 7.50 (d, 2H, J = 9.0, 2-H-Ar), 6.83 (d, 1H, J = 15.9, Ar-C*H*=CH-pyridinium ring), 6.68 (d, 2H, J = 9.0, 3-Ar), 5.73 (dt, 1H, J = 15.4, 6.8, 5-H), 5.45 (dd, 1H, J = 15.4, 6.8, 4-H), 4.75 (br s, 1H, 3-OH), 4.54 (m, 3H, 3-OH and C(6)H_2-pyridinium ring), 4.35 (m, 1H, 3-H), 3.90 (m, 2H, 1-Ha and 2-H), 3.67 (d, 2H, J = 7.7, 1-Hb), 3.06 (s, 6H, N(CH_3)$_2$), 2.43 (m, 2H, COCH_2), 2.1 (m, 2H, C(5)H_2C(6)H_2-pyridinium ring), 1.90 (q, 2H, J = 7.2, C(6)H_2), 1.78 (m, 2H, $COCH_2CH_2$), 1.48 (m, 2H, $COCH_2CH_2CH_2$), 1.23 (m, 22H, CH_2), 0.86 (t, 3H, J = 7. 1, CH_3); ESI-MS (CH_3OH, relative intensity, %) m/z 620.4 (M^+, 100). Calcd for $[C_{39}H_{62}N_3O_3]^+$ m/z 620.5. Anal. Calcd for $C_{39}H_{62}BrN_3O_3$ (700.8): C, 66.84; H, 8.92; N, 6.00; Br, 11.40. Found: C, 63.56; H, 8.75; N, 5.64; Br, 11.30.

4.1.2.15. D-*erythro*-2-*N*-(1′-Octylnicotinoyl)-sphingosine bromide (LCL275). Prepared from D-*erythro*-2-*N*-nicotinoyl-sphingosine (**19**, 202 mg, 0.5 mmol) and octyl bromide (2 mL) according to the Procedure C with the reaction time extended to 8 h. The crude product was washed with warm *n*-hexane and crystallized twice from ethyl acetate to give pure **LCL275** (174 mg, 58%) as a pale yellow powder, mp 117–118 °C; TLC ($CHCl_3$–$(CH_3)_2CO$–MeOH–CH_3COOH–H_2O, 20:8:6:2:1, v/v) R_f 0.45; RP TLC (C18 Silica, CH_3CN–MeOH–1 M NH_4Cl(aq), 4:1:1.5, v/v) R_f 0.47; $[\alpha]_D^{20}$ +4.60° (c 1, MeOH); $[\alpha]_{365}^{20}$ +20.1° (c 1, MeOH); ^{1}H NMR (500 MHz, $CDCl_3$) δ 10.53 (s, 1H, 2-H_{Py}), 9.11 (d, 1H, J = 8.1, 4-H_{Py}), 9.07 (d, 1H, J = 7.4, NH), 8.73 (d, 1H, J = 6.0, 6-H_{Py}) 8.08 (dd, 1H, J = 8.1 and 6.1, 5-H_{Py}), 5.85 (dtd, 1H, J = 15.4, 6.6, 1.2, 5-H), 5.45 (ddt, 1H, J = 15.4, 7.1, 1.2, 4-H), 4.81 (t, 2H, J = 7.6, CH_2-pyridinium ring), 4.56 (m, 1H, 3-H), 4.38 (br s, 1H, 3-OH), 4.2 (br s, 1H, 1-OH), 4.07 (dd, 1H, J = 12.1, 5.7, 1-Ha), 4.00 (m, 1H, 2-H), 3.90 (dd, 1H, J = 12.1, 2.3, 1-Hb), 2.10 (m, 2H, CH_2 CH_2-pyridinium ring), 2.03

(q, 2H, J = 7.2, C(6)H_2), 1.35 (m, 6H, C(7)H_2, CH_2 CH_2 CH_2-pyridinium ring and C$H_2$$CH_2$$CH_2$$CH_2$-pyridinium ring), 1.24 (m, 26H, CH_2), 0.87 (t, 3H, J = 6.9, CH_3), 0.86 (t, 3H, J = 7.1, CH_3); (CD_3OD) δ 9.42 (s, 1H, 2-H_{Py}), 9.12 (dt, 1H, J = 6.1, 1,3, 4-H_{Py}), 9.07 (dt, 1H, J = 8.2, 1,4, 6-H_{Py}), 8.08 (dd, 1H, J = 8.0, 6.2, 5-H_{Py}), 5.73 (dtd, 1H, J = 15.4, 6.6, 1.1, 5-H), 5.55 (ddt, 1H, J = 15.4, 7.1, 1.1, 4-H), 4.68 (t, 2H, J = 7.7, CH_2-pyridinium ring), 4.21 (t, 1H, J = 6.8, 3-H), 4.16 (m, 1H, 2-H), 3.86 (dd, 1H, J = 11.5, 4.2, 1-Ha), 3.78 (dd, 1H, J = 11.5, 7.2, 1-Hb), 2.02 (m, 4H, C$H_2$$CH_2$-pyridinium ring and C(6)H_2), 1.30 (m, 32H, CH_2), 0.89 (t, 3H, J = 6.9, CH_3), 0.88 (t, 3H, J = 7.1, CH_3); (D_2O) δ 10.50 (s, 1H, 2-H_{Py}), 9.35 (d, 1H, J = 6.1, 1,3, 4-H_{Py}), 9.15 (t, 1H, J = 7.1, 6-H_{Py}), 8.46 (dd, 1H, J = 8.0, 6.1, 5-H_{Py}), 5.92 (dtd, 1H, J = 15.2, 6.3, 1.1, 5-H), 5.62 (ddt, 1H, J = 15.2, 7.2, 1.1, 4-H), 4.99 (t, 2H, J = 7.0, CH_2-pyridinium ring), 4.41 (t, 1H, J = 8.0, 3-H), 4.27 (m, 1H, 2-H), 4.10 (dd, 1H, J = 11.7, 3.4, 1-Ha), 4.02 (dd, 1H, J = 11.7, 6.0, 1-Hb), 2.18 (m, 2H, C(6)H_2), 2.0 (m, 2H, C$H_2$$CH_2$-pyridinium ring), 1.25 (m, 32H, CH_2), 0.84 (t, 3H, J = 6.9, CH_3), 0.80 (t, 3H, J = 7.1, CH_3); ^{13}C-NMR (CD_3OD) δ 163.8 (C=O), 147.5 ($C2_{Py}$), 145.9 ($C6_{Py}$), 144.9 ($C3_{Py}$), 136.8 ($C4_{Py}$), 135.1(*C4*=C5), 131.0 (C4=*C5*), 129.4($C5_{Py}$), 73.6 (C3), 63.7 (*C1*-pyridinium-ring), 61.8 (C1), 58.5 (C2), 33.5(C4=C5*C6*), 33.2 (C4=C5C6*C*7 or C4=C5C6C7*C*8), 33.0 (C4=C5 C6*C*7 or C4=C5C6C7*C*8), 32.7 (*C*2C1-pyridinium ring), 30.91, 30.88, 30.85, 30.74, 30.6, 30.53, 30,41, 30.3 and 30.25 (C8–C16 and C4–C6), 27.3 (*C*3C2C1-pyridinium ring), 23.85 (C17), 23.78 (*C7*CH_3), 14.55 (CH_3), 14.51 (CH_3); ESI-MS (CH_3OH, relative intensity, %) *m/z* 1515.3 ($[2M+Br]^+$, 65), 517.5 (M^+, 100). Calcd for $[C_{32}H_{57}N_2O_3]^+$ *m/z* 517.4. Anal. Calcd for $C_{32}H_{57}BrN_2O_3$ (597.7): C, 64.30; H, 9.61; N, 4.69; Br, 13.37. Found: C, 64.05; H, 9.57; N, 4.71; Br, 13.24.

4.1.2.16. D-*erythro*-2-*N*-[3′-[3″-(1″-Butyl)-pyridinium]-propionoyl]-sphingosine bromide (LCL277). Prepared from D-*erythro*-2-*N*-[3′-(3″-pyridyl)-propionoyl]-sphingosine (**20**) and butyl bromide in 68% yield as **LCL275** from **19**. Analytical sample of **LCL277** was prepared by crystallization from ethyl acetate as a pale yellow powder, mp 134–135 °C; TLC ($CHCl_3$–$(CH_3)_2CO$–MeOH–CH_3COOH–H_2O, 20:8:6:2:1, v/v) R_f 0.21; RP TLC (C18 Silica, CH_3CN–MeOH–1 M NH_4Cl(aq), 4:1:1.5, v/v) R_f 0.43; $[\alpha]_D^{22}$ −10.0° (*c* 1, MeOH); $[\alpha]_{365}^{22}$ −37.1° (*c* 1, MeOH); ^{1}H NMR (500 MHz, $CDCl_3$) δ 9.39 (s, 1H, 2-H_{Py}), 8.45 (d, 1H, J = 6.1, 6-H_{Py}), 8.32 (d, 1H, J = 7.8, 4-H_{Py}), 8.17(d, 1H, J = 6.9, NH), 7.85 (dd, 1H, J = 7.8 and 6.1, 5-H_{Py}), 5.85 (dtd, 1H, J = 15.2, 6.7, 1.1, 5-H), 5.45 (ddt, 1H, J = 15.2, 7.1, 1.1, 4-H), 4.81 (m, 2H, CH_2-pyridinium ring), 4.12 (m, 1H, 3-H), 3.76 (dd, 1H, J = 12.1, 5.8, 1-Ha), 3.63 (m, 1H, 2-H), 3.52 (dd, 1H, J = 12.1, 2.4, 1-Hb), 3.27 (m, 2H, COCH_2), 3.05 (m, 1H, $COCH_2CH_2$), 2.95 (m, 1H, $COCH_2CH_2$), 2.0 (m, 4H, C$H_2$$CH_2$-pyridinium ring and C(6)H_2), 1.43 (m, 2H, CH_2)CH_2CH_2-pyridinium ring), 1.31 (m, 2H, C(7)H_2), 1.24 (m, 20H, CH_2), 0.98 (t, 3H, J = 7.3, CH_3), 0.86 (t, 3H, J = 7.2, CH_3); (CD_3OD) δ 8.89 (s, 1H, 2-H_{Py}), 8.87 (d, 1H, J = 6.1, 6-H_{Py}), 8.46 (d, 1H, J = 7.9, 4-H_{Py}), 7.99 (dd, 1H, J = 7.9, 6.1, 5-H_{Py}), 5.68 (dtd, 1H, J = 15.2, 6.8, 1.1, 5-H), 5.43 (ddt, 1H, J = 15.2, 7.0, 1.1, 4-H), 4.58 (t, 2H, J = 7.6, CH_2-pyridinium ring), 4.03 (t, 1H, J = 7.0, 3-H), 3.86 (m, 1H, 2-H), 3.63 (dd, 1H, J = 11.2, 4.2, 1-Ha), 3.56 (dd, 1H, J = 11.2, 6.9, 1-Hb), 3.14 (m, 2H, $COCH_2$), 2.66 (m, 2H, $COCH_2CH_2$), 2.0 (m, 4H, C$H_2$$CH_2$-pyridinium ring, C(6)$H_2$), 1.40 (m, 4H, C(7)$H_2$, C$H_2$$CH_2$$CH_2$-pyridinium ring), 1.27 (m, 20H, CH_2), 1.0 (t, 3H, J = 7.4, CH_3), 0.89 (t, 3H, J = 6.9, CH_3); (D_2O) δ 8.91 βσ, 1H, 2-H_{Py}), 8.87 (d, 1H, J = 6.0, 6-H_{Py}), 8.58 (d, 1H, J = 8.0, 4-H_{Py}), 8.13 (dd, 1H, J = 8.0, 6.0, 5-H_{Py}), 5.83 (dtd, 1H, J = 15.2, 6.8, 1.1, 5-H), 5.59 (ddt, 1H, J = 15.2, 7.0, 1.1, 4-H), 4.72 (t, 2H,J = 7.3, CH_2-pyridinium ring), 4.26 (t, 1H, J = 5.7, 3-H), 3.99 (m, 1H, 2-H), 3.77 (dd, 1H, J = 11.1, 4.1, 1-Ha), 3.73 (dd, 1H, J = 11.1, 6.6, 1-Hb), 3.27 (m, 2H, $COCH_2$), 2.85 (m, 2H, $COCH_2CH_2$), 2.07 (m, 4H, C$H_2$$CH_2$-pyridinium ring, C(6)$H_2$), 1.45 (m, 4H, C(7)$H_2$, C$H_2$$CH_2$$CH_2$- pyridinium ring), 1.33 (m, 20H, CH_2), 1.02 (t, 3H, J = 7.2, CH_3), 0.93 (t, 3H, J = 6.7, CH_3); ESI-MS (CH_3OH, relative intensity, %) *m/z* 489.5 (M^+, 100). Calcd for $[C_{30}H_{53}N_2O_3]^+$ *m/z* 489.4. Anal. Calcd for $C_{30}H_{53}BrN_2O_3$ (569.7): C, 63.25; H, 9.38; N, 4.92; Br, 14.03. Found: C, 63.03; H, 9.47; N, 4.86; Br, 14.28.

4.1.3. Solubility of CCPS analogs and Cers in water. The assay was carried out according to the published method used for the solubility assessment of CPB and its analogs.[82] Saturated solutions of Cers and CCPS analogs were prepared by dissolving a known amount of lipid (generally 25 mg of CCPS lipid or 4 mg of Cer) in the appropriate volume of double distilled water. The solubility measurements were performed in a constant-temperature shaking bath by increasing and decreasing temperature between 20 and 40 °C. Solubility of C2-, C6-, and C16-Cers was measured by a direct infusion of the aqueous solution of lipids into LC–MS system. The obtained analytical results were processed as reported.[21,95]

4.1.4. Stability assays. Samples of **LCL29**, **30**, **88**, and **150** were dissolved in phosphate buffer solutions (pH 4.5, 7.4, and 8.5) and allowed to stand at 40 °C over a period of 48 h. After that period of time, the lipid solutions were analyzed by RP TLC and LC–MS as described below.

4.1.5. Molecular hydrophobicity. The flow rates of CCPS analogs (R_f values) were determined by RP-TLC using C18-silica gel plates and acetonitrile–methanol–1 M NH_4Br(aq) (4:1:1.5, v/v/v) as the eluent. The molecular hydrophobicity (R_M) values were calculated from the following equation: $R_M = \log(1/R_f - 1)$.[65]

4.2. Biology

4.2.1. Cell culture. MCF7 cells (breast adenocarcinoma, pleural effusion) were purchased from American type Culture Collection (ATCC) (Rockville, MD, USA), grown in RPMI 1640 media (Life Technologies, Inc.) supplemented with 10% fetal calf serum (FCS) (Summit Biotechnology, CO, USA), and maintained under stan-

dard incubator conditions (humidified atmosphere 95% air, 5% CO_2 37 °C). A parallel set of cells was used to determine cell proliferation and to prepare lipid extracts for MS analysis.

4.2.2. Cell proliferation. Cells were seeded at a density of ≈50% corresponding to 1×10^6 cells, in 10 mL of 10% FCS and after an overnight incubation were treated with LCL compounds at concentration 0–20 μM in ethanol (ethanol level was kept below 0.1%) and the changes in cell numbers after 24 or 48 h were determined and expressed as a percentage of the untreated controls. Briefly, media were removed, cells were washed twice with PBS, detached using 1% trypsin, and centrifuged at 800 rpm. Cell pellets were resuspended in PBS and Trypan blue (Sigma Chemicals, St. Louis, MO, USA) was added (1:1 dilution). Under light microscope, the percentage of unstained and stained cells was assessed.

4.2.3. LC–MS analysis of endogenous Cers and cellular level of CCPS and dhCCPS analogs. Advanced analyses of Cers and ceramidoids were performed by the Lipidomics Core at MUSC on Thermo Finnigan TSQ 7000, triple-stage quadrupole mass spectrometer operating in a Multiple Reaction Monitoring (MRM) positive ionization mode as described.[95] Quantitative analysis of the cellular level of CCPS and dhCCPS analogs was based on the calibration curves generated by spiking an artificial matrix with the known amounts of the target standards and an equal amount of the internal standards (IS). The target analyte to IS peak area ratios from the samples were similarly normalized to their respective IS and compared to the calibration curves using a linear regression model.

Acknowledgments

This work was supported by NIH Grant Nos. RR17677, C06RR018823 and AG16583 as well as by NCI Grant No. IPO1CA097132.

References and notes

1. Obeid, L. M.; Linardic, C. M.; Karolak, L. A.; Hannun, Y. A. *Science.* **1993**, *259*, 1769.
2. Pettus, B. J.; Chalfant, C. E.; Hannun, Y. A. *Biochim. Biophys. Acta* **2002**, *1585*, 114.
3. Ruvolo, P. P. *Pharmacol. Res.* **2003**, *47*, 383.
4. Thomas, R. L.; Matsko, C. M.; Lotze, M. T.; Amoscatov, A. A. *J. Biol. Chem.* **1999**, *247*, 30580.
5. Caricchio, R.; Adamio, L. D.; Cohen, P. L. *Cell Death Differ.* **2002**, *9*, 574.
6. Basnakian, A. G.; Ueda, N.; Hong, X.; Galitovsky, V. E.; Yin, X.; Shah, S. V. *Am. J. Physiol. Renal. Physiol.* **2005**, *288*, 308.
7. Samsel, L.; Zaidel, G.; Drumgoole, H. M.; Jelovac, D.; Drachenberg, C.; Rhee, J. G.; Brodie, A. M. H.; Bielawska, B.; Smyth, M. J. *Prostate* **2004**, *58*, 382.
8. Bielawska, A.; Greenberg, M. S.; Perry, D.; Jayadev, S.; Shayman, J. A.; McKay, C.; Hannun, Y. A. *J. Biol. Chem.* **1996**, *271*, 12646.
9. Selzner, M.; Bielawska, A.; Morse, M. A.; Rudiger, H. A.; Sindram, D.; Hannun, Y. H.; Clavien, P. A. *Cancer Res.* **2001**, *61*, 1233.
10. Gouaze, V.; Liu, Y.-Y.; Prickett, C. S.; Yu, J. Y.; Giuliano, A. E.; Cabot, M. C. *Cancer Res.* **2005**, *65*, 3861.
11. Ogretmen, B.; Pettus, B. J.; Rossi, M. J.; Wood, R.; Usta, J.; Szulc, Z.; Bielawska, A.; Obeid, L. M.; Hannun, Y. A. *J. Biol. Chem* **2002**, *277*, 12960.
12. Lopez-Marure, R.; Gutierrez, G.; Maendoza, C.; Ventura, J. L.; Sanchez, L.; Maldonado, E. R.; Zentella, A.; Montano, L. F. *Biochem. Biophys. Res. Commun.* **2002**, *293*, 1028.
13. Fillet, M.; Bentires-Alj, M.; Deregowski, V.; Griemers, R.; Gielen, J.; Piette, J.; Bours, V.; Merville, M.-P. *Biochem. Pharmacol.* **2003**, *65*, 1633.
14. Chalfant, C. E.; Szulc, Z. M.; Roddy, P.; Bielawska, A.; Hannun, Y. A. *J. Lipid Res.* **2003**, *45*, 496.
15. Lozano, J.; Berra, E.; Municio, M. M.; Diaz-Meco, M. T.; Dominguez, I.; Sanz, L.; Moscat, J. *J. Biol. Chem.* **1994**, *269*, 19200.
16. Wickel, M.; Heinrich, M.; Weber, T.; Brunner, J.; Kronke, M.; Schutze, S. *Biochem. Soc. Trans.* **1999**, *27*, 399.
17. Ogretmen, B.; Kraveka, J. M.; Schady, D.; Usta, J.; Hannun, Y. A.; Obeid, L. *J. Biol. Chem.* **2001**, *276*, 32506.
18. Birbes, H.; Bawab, S. E.; Obeid, L. M.; Hannun, Y. A. . *Adv. Enzyme Regul.* **2002**, *42*, 113.
19. Lucci, A.; Giuliamo, A. E.; Han, T. Y.; Dinur, T.; Liu, Y. Y.; Senchenkov, A.; Cabot, M. C. *Int. J. Oncol.* **1999**, *15*, 535.
20. Tserng, F.-Y.; Griffin, R. L. *Biochem. J.* **2004**, *380*, 715.
21. Sultan, I.; Senkal, C. E.; Ponnusamy, S.; Bielawski, J.; Szulc, Z. M.; Bielawska, A.; Hannun, Y. A.; Ogretmen, B. *Biochem. J.* **2006**, *393*, 513.
22. Takeda, S.; Mitsutake, S.; Tsuji, K.; Igarashi, Y. *J. Biochem.* **2006**, *139*, 255.
23. Mimeault, M. *FEBS Lett.* **2002**, *530*, 9.
24. Sullards, M. C.; Wang, E.; Peng, Q.; Merrill, A. H. *Cell Mol. Biol.* **2003**, *49*, 789.
25. Ogretmen, B.; Hannun, Y. A. *Nat. Rev. Cancer* **2004**, *4*, 604.
26. Vaknin, D.; Kelley, M. S. *Biophys. J.* **2000**, *79*, 2616.
27. Carrer, D. C.; Maggio, B. *J. Lipid. Res.* **1999**, *40*, 1978.
28. Brockman, H. L.; Momse, M. M.; Brown, R. E.; He, L.; Chun, J.; Byun, H.-S.; Bittman, R. *Biophys. J.* **2004**, *87*, 1722.
29. Sot, J.; Aranda, F. J.; Collado, M.-I.; Goni, F. M.; Alonso, A. *Biophys. J.* **2005**, *88*, 3368.
30. Sot, J.; Goni, F. M.; Alonso, A. *Biochim. Biophys. Acta* **2005**, *1711*, 12.
31. Zhang, Ji. L.; Uematsu, S.; Akahori, Y.; Hirabayashi, Y. *FEBS Lett.* **1995**, *358*, 211.
32. Kolesnick, R.; Hannun, Y. A. *Trends Bochem. Sci.* **1999**, *24*, 224.
33. Paris, F.; Grassme, H.; Cremesti, A.; Zager, J.; Fong, Y.; Halmovitz-Friedman, A.; Fuks, Z.; Gulbin, E.; Kolesnick, R. *J. Biol. Chem.* **2001**, *276*, 8297.
34. Tsering, K. Y.; Griffin, L. *Biochem. J.* **2004**, *380*, 715.
35. Urbina, P.; Alonso, A.; Contreras, F. X.; Goni, F. M.; Lopez, D. J.; Montes, L. R.; Sot, J. *Chem. Phys. Lipids* **2006**, *139*, 107.
36. Babia, T.; Ledesma, M. D.; Saffrich, R.; Kok, J. K.; Dotti, C. G.; Egea, G. *Traffic* **2001**, *2*, 395.
37. Hu, W.; Xu, R.; Zhang, G.; Jin, J.; Szulc, Z.; Bielawski, J.; Hannun, Y. A.; Obeid, L.; Mao, C. *Mol. Biol. Cell* **2005**, *16*, 1555.
38. Stover, T.; Kester, M. *J. Pharm. Exp. Ther.* **2003**, *307*, 468.
39. Shabbits, J. A.; Mayer, L. D. *Anticancer Res.* **2003**, *23*, 3663.

40. Shabbits, J. A.; Mayer, L. D. *Biochem. Biophys. Acta* **2003**, *1612*, 98.
41. Stover, T. C.; Sharma, A.; Roberstson, G. P.; Kester, M. *Clin. Cancer Res.* **2005**, *11*, 3465.
42. Futerman, A. H.; Hannun, Y. A. *EMBO Rep.* **2004**, *5*, 777.
43. Bionda, C.; Portoukalian, J.; Schmitt, D.; Rodrigez-Lafrasse, C.; Ardail, D. *Biochem. J.* **2004**, *382*, 527.
44. Modica-Napolitano, J. S.; Aprille, J. R. *Adv. Drug Deliv. Rev.* **2001**, *49*, 63.
45. Birbes, H.; El Bawab, S.; Hannun, Y. A.; Obeid, L. *FASEB J.* **2001**, *14*, 2669.
46. Bribes, H.; Luberto, C.; Hsu, Y. T.; El Bawab, S.; Hannun, Y. A.; Obeid, L. *Biochem. J.* **2005**, *386*, 445.
47. von Haefen, C.; Wieder, T.; Gillissen, B.; Starck, L.; Graupner, V.; Dorken, B.; Daniel, P. T. *Oncogene* **2002**, *21*, 4009.
48. Siskind, L. J. *J. Bioenerg. Biomembr.* **2005**, *37*, 143.
49. Di Poala, M.; Cocco, T.; Lorusso, M. *Biochemistry* **2000**, *39*, 6660.
50. Stoica, B. A.; Movsesyan, V. A.; Knoblach, S. M.; Faden, A. I. *Mol. Cell Neurosci.* **2005**, *29*, 355.
51. Kandela, I. K.; Lee, W.; Indig, G. L. *Biotech. Histochem.* **2003**, *78*, 157.
52. Trapp, S.; Horobin, R. W. *Eur. Biophys. J.* **2005**, *34*, 959.
53. Asin-Cayuela, J.; Manas, A.-R. B.; James, A. M.; Smith, R. A. J.; Murphy, P. M. *FEBS Lett.* **2004**, *571*, 9.
54. Sheu, S.-S.; Nauduri, D.; Anders, M. W. *Biochem. Biophys. Acta* **2006**, *1762*, 256.
55. Ross, G. F.; Smith, P. M.; McGregor, A.; Turnbull, D. M.; Lightowlers, R. N. *Bioconj. Chem.* **2003**, *14*, 962.
56. Fantin, V. R.; Berardi, M. J.; Scorrano, L.; Korsmeyer, S. J.; Leder, P. *Cancer Cell* **2002**, *2*, 29.
57. Rosania, G. R.; Lee, J. W.; Ding, L.; Yoon, H.-S.; Chang, Y.-T. *J. Am. Chem. Soc.* **2003**, *125*, 1130.
58. Sturla, M.; Masini, M. A.; Prato, P.; Grattarola; Uva, B. *Cell Tissue Res.* **2001**, *303*, 351.
59. Dias, N.; Bailly, C. *Biochem. Pharmacol.* **2005**, *70*, 1.
60. Palin, R.; Clark, J. K.; Cowley, P.; Muir, A. W.; Pow, E.; Prosser, A. B.; Taylor, R.; Zhang, M.-Q. *Bioorg. Med. Chem. Lett.* **2002**, *12*, 2569.
61. Walker, S.; Sofia, M. J.; Axelrod, H. R. *Adv. Drug Deliv. Rev.* **1998**, *30*, 61.
62. Usta, J.; El-Bawab, S.; Szulc, Z.; Hannun, Y. A.; Bielawska, A. *Biochemistry* **2001**, *40*, 9657.
63. Chalfant, C. E.; Szulc, Z. M.; Roddy, P.; Bielawska, A.; Hannun, Y. A. *J. Lipid Res.* **2004**, *45*, 496.
64. Wijesinghe, D. S.; Massiello, A.; Subramanian, P.; Szulc, Z.; Bielawska, A.; Chalfant, C. *J. Lipid Res.* **2005**, *46*, 2706.
65. Shirai, A.; Maeda, T.; Nagamune, H.; Matsuki, H.; Kanashina, S.; Kourai, H. *Eur. J. Med. Chem.* **2005**, *40*, 113.
66. Ivanov, I.; Vemparala, S.; Pophristic, V.; Kuroda, K.; DeGrado, W. F.; McCammon, A.; Klein, M. L. *J. Am. Chem. Soc.* **2006**, *128*, 1778.
67. Scarzello, M.; Smisterova, J.; Wagenaar, A.; Stuart, M. C.; Hoekstra, D.; Engberts, J. B. F. N.; Hulst, R. *J. Am. Chem. Soc.* **2005**, *127*, 10420.
68. Teruya, T.; Kobayashi, K.; Suenaga, K.; Kigoshi, H. *J. Nat. Prod.* **2006**, *69*, 135.
69. Kloc, K.; Szulc, Z.; Mlochowski, J. *Can. J. Chem.* **1979**, *57*, 1506.
70. Hulst, R.; Muizebelt, I.; Oosting, P.; van der Pol, C.; Wagenaar, A.; Sÿmisterova, J.; Bulten, E.; Driessen, C.; Hoekstra, D.; Engberts, J. B. *Eur. J. Org. Chem.* **2004**, *4*, 835.
71. Zu, Y.; Li, Q.; Fu, Y.; Wang, W. *Bioorg. Med. Chem. Lett.* **2004**, *14*, 4023.
72. Haldar, J.; Kondaiah, P.; Bhattacharya, S. *J. Med. Chem.* **2005**, *48*, 3823.
73. Novgorodov, S. A.; Szulc, Z. M.; Luberto, C.; Jones, J. J.; Bielawski, J.; Bielawska, A.; Hannun, Y. A.; Obeid, L. *J. Biol. Chem.* **2005**, *280*, 16096.
74. Rossi, M. J.; Sundararaj, K.; Koybasi, S.; Phillips, M. S.; Szulc, Z.; Bielawska, A.; Day, T. A.; Obeid, L.; Hannun, Y. A.; Ogretmen, B. *Otalaryngol. Head Neck Surg.* **2005**, *132*, 55.
75. Senkal, C.; Ponnusamy, S.; Rossi, M.; Sundararaj, K.; Szulc, Z.; Bielawski, J.; Bielawska, A.; Meyer, M.; Cobanoglu, B.; Koybasi, S.; Sinha, D.; Day, T. A.; Obeid, L.; Hannun, Y. A.; Ogretmen, B. *J. Pharmacol. Exp. Ther.* **2006**, *317*, 1188.
76. Dindo, D.; Dahm, F.; Szulc, Z.; Bielawska, A.; Obeid, L. M.; Hannun, Y. A.; Graf, R.; Clavien, P. A. *Mol. Cancer Ther.* **2006**, *5*, 1520.
77. Quagliotto, P.; Viscardi, G.; Barolo, C.; Barni, E.; Bellinvia, S.; Fisicaro, E.; Compari, C. *J. Org. Chem.* **2003**, *68*, 7651.
78. Janout, V.; Regen, S. L. *J. Am. Chem. Soc.* **2005**, *127*, 22.
79. Yu, H.; Narusawa, H.; Itoh, K.; Oshi, A.; Yoshino, N.; Ohbu, K.; Shirikawa, T.; Fukuda, K.; Fuji, M.; Kato, T.; Seimiya, T. *J. Colloid Interface Sci.* **2000**, *229*, 375.
80. Bieberich, E.; Hu, B.; Silva, J.; MacKinnon, S.; Yu, R. K.; Fillmore, H.; Broaddus, W. C.; Ottenbrite, R. M. *Cancer Lett.* **2002**, *181*, 55.
81. Villard, R.; Hammache, D.; Delapierre, G.; Fotiadu, F.; Buono, G.; Fantini, J. *Chem. Bio. Chem.* **2002**, *3*, 517.
82. Adam, N. K.; Pankhurst, K. G. A. *Trans. Faraday Soc.* **1946**, *42*, 523.
83. Li, L.; Tang, X.; Taylor, K. G.; DuPre, D. B.; Yappert, C. *Biophys. J.* **2002**, *82*, 2067.
84. Chen, J. Z.; Han, X.-W.; Xie, X.-Q. *Life Sci.* **2005**, *76*, 2053.
85. Higashibayashi, S.; Kishi, Y. *Tetrahedron* **2004**, *60*, 11977.
86. Cloran, F.; Carmichael, I.; Serianni, A. S. *J. Am. Chem. Soc.* **2001**, *123*, 4781.
87. Kover, K. E.; Feher, K. *J. Mag. Reson.* **2004**, *168*, 307.
88. Thiele, C. M.; Berger, S. *Org. Lett.* **2003**, *5*, 705.
89. Lazaridis, T. *Acc. Chem. Res.* **2001**, *34*, 931.
90. Herbert, R. H.; Gerhard, U.; Mortishire-Smith, R. J.; Thomas, S. R.; Hollingworth, G. *Magn. Reson. Chem.* **2005**, *43*, 658.
91. Bakshi, M. S.; Sood, R. *Colloids Surf. A: Physicochem. Eng. Aspects* **2004**, *244*, 159.
92. Garner, P.; Park, J. M.; Malecki, E. *J. Org. Chem.* **1988**, *53*, 4395.
93. Ninkar, S.; Menaldino, D.; Merrill, A. H.; Liotta, D. *Tetrahedron Lett.* **1988**, *29*, 3037.
94. Herold, P. E. *Helv. Chim. Acta* **1988**, *71*, 354.
95. Bielawski, J.; Szulc. Z. M.; Hannun, Y.A.; Bielawska, A. *Methods, cancer Ther.* **2006**, *39*, 82.